Chemical Reviews

Volume 76, Number 4 August 1976

Electron Attachment to Molecules in Dense Gases ("Quasi-Liquids")

L. G. CHRISTOPHOROU*

Health Physics Division, Oak Ridge National Laboratory, Oak Ridge, Tennessee

Received May 23, 1975 (Revised Manuscript Received July 17, 1975)

Contents

I. Introduction

A crucial step in our efforts to develop not only a coherent picture of radiation interaction with matter, but also an understanding of radiation effects and mechanisms, is to relate the often abundant knowledge on isolated molecules (low-pressure gases) to that in the condensed phase. There is a need for an understanding of the environmental influences on the elementary processes which accompany the interaction of radiation with matter. Moreover, to understand the roles of the physical and chemical properties of molecules in biological reactions, we must know how these "isolated-molecule" properties change as a molecule finds itself in gradually denser and denser gaseous and, finally, in condensed-phase environments.

Such "intermediate" or "interphase" studies, especially on electron–molecule interaction processes, have attracted considerable interest recently. They provide an insight as to the effects of the density and the nature of the environment on the fundamental electron–molecule interaction processes at densities intermediate to those corresponding to low-pressure gases and liquids and on the gradual transition from "isolated-molecule" to "condensed-phase" behavior. Accurate measurements of the rates and the cross sections for attachment of slow electrons to molecules in high-pressure gases are quite helpful in elucidating the collision kinetics of electron–molecule interaction processes and therefore in unifying the modeling of gas-phase phenomena with those in the liquid phase.

It is the purpose of this paper to review, expand, and elaborate on current work on electron attachment to molecules in "quasi-liquid" (high-pressure) media. Similar work on electron motion in low- and high-pressure gases and liquids has been reviewed recently by the author.[1]

II. Experimental Methods

In such studies we are obviously dealing with electrons having a wide spread in their kinetic energies (i.e., with electron-swarms), and, by necessity, we have to work with binary gas mixtures whereby the compound under investigation is mixed in very small proportions with an abundant non-electron-attaching ("carrier") gas. Furthermore, as a rule, one has to restrict himself to a limited number of carrier gases for which the electron energy distribution functions are known as a function of the experimental parameter E/P, the pressure-reduced electric field. Knowledge of the electron energy distribution functions $f(\epsilon,E/P)$ or $f(\epsilon,\langle\epsilon\rangle)$, where $\langle\epsilon\rangle$ is the mean electron energy which corresponds to E/P, is necessary for a meaningful physical analysis of the raw experimental data. Even for such carrier gases, experiments at high pressures (1 to ~100 atm) are faced with serious difficulties,[2,3] and one should exercise extreme caution to consider possible changes in the electron swarm drift velocity with gas density and divergences of the carrier gases from "ideal-gas-law" behavior and also to ensure that, in the ensuing analyses of the high-pressure data, $f(\epsilon,E/P)$

* Also, Department of Physics, University of Tennessee, Knoxville, Tenn. 37916.

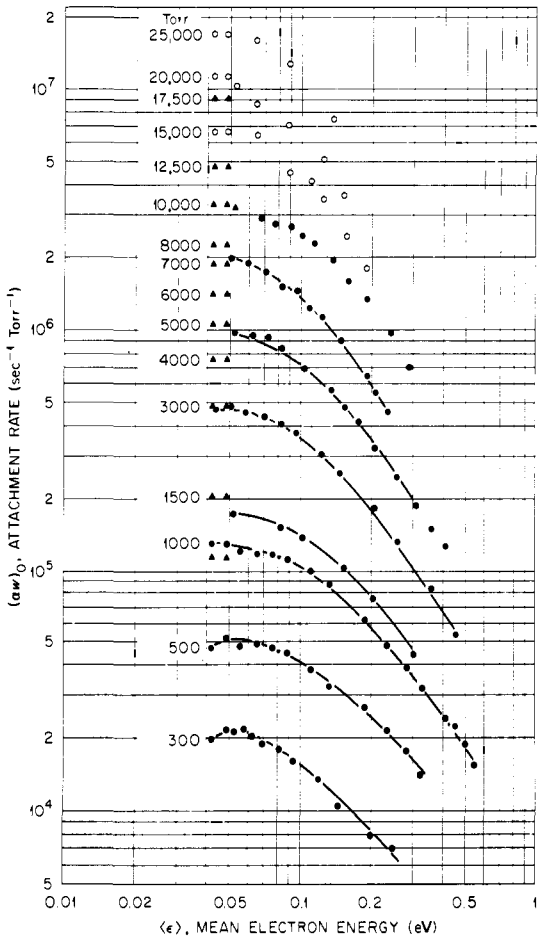

Figure 1. Attachment rate $(\alpha w)_0$ as a function of mean electron energy, $\langle\epsilon\rangle$ for O_2 in N_2, for N_2 pressures between 300 and 25,000 Torr. ●, ref 2; ▲ and O, ref 3. $(\alpha w)_0$ represents the measured attachment rate when $P_{O_2} \rightarrow 0$ Torr.

is not altered from that which is characteristic of the low-pressure gas.

In the experimental work to be discussed in the following sections, Ar, N_2, C_2H_4, and C_2H_6 were used as carrier gases. The former two can be considered as ideal gases up to the highest pressures so far employed in these studies (~50 000 Torr), but the latter two cease to be incompressible at relatively low pressures. In this latter case the compressibility factor z is <1 and the measured pressures, P_m, are divided by z so that the quantity $P' = P_m/z$ is obtained for which

$$E/P' \propto E/N \tag{1}$$

where N is the number density (number of molecules per cm^3).

The swarm method has been reviewed earlier at length.[4] Details on the extension of these studies to the "quasi-liquid" regime have likewise been given.[2,3] Furthermore, Christophorou et al.[5] described a method referred to as the "swarm-unfolding technique" which allows determination of the attachment cross section $\sigma_a(\epsilon)$ as a function of electron energy ϵ, virtually at any gas density for which $f(\epsilon,E/P)$ is known and the attachment rate αw has been measured over a wide and convenient range of E/P. The rate αw (α is the attachment coefficient and w is the electron-swarm drift velocity) is a quantity which is averaged over $f(\epsilon,E/P)$. Hence we may write

$$\alpha w(\langle\epsilon\rangle_j) = \int_0^\infty \alpha w(\epsilon) f(\epsilon,\langle\epsilon\rangle_j)\, d\epsilon \tag{2}$$

where $\alpha w(\langle\epsilon\rangle_j)$ is the value of the rate at the mean energy $\langle\epsilon\rangle_j$ (i.e., at the jth value of E/P), $f(\epsilon,\langle\epsilon\rangle_j)$ is the electron energy distribution function that corresponds to $\langle\epsilon\rangle_j$, and $\alpha w(\epsilon)$ is the value of the monoenergetic attachment rate at the energy ϵ (i.e., the value of the attachment rate that would be measured had all the electrons in the swarm had the same energy, ϵ). Equation 2 forms the basis of the "swarm unfolding technique", and Christophorou et al. have described an iterative procedure which allows $\alpha w(\epsilon)$ to be unfolded from the measured functions $\alpha w(\langle\epsilon\rangle_j)$ using the corresponding known functions $f(\epsilon,\langle\epsilon\rangle_j)$. Once $\alpha w(\epsilon)$ is determined, the attachment cross section $\sigma_a(\epsilon)$ is obtained from

$$\sigma_a(\epsilon) = \alpha w(\epsilon)/N_0(2/m)^{1/2}\epsilon^{1/2} \tag{3}$$

where m is the electron mass and N_0 is the number of molecules per cm^3 per Torr.

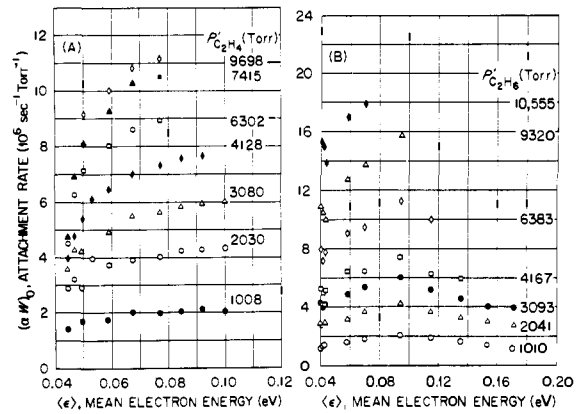

Figure 2. Attachment rate $(\alpha w)_0$ as a function of the mean electron energy $\langle\epsilon\rangle$ for (A) O_2 in C_2H_4 and (B) O_2 in C_2H_6 at the indicated total pressures.

III. O_2

Electron attachment to O_2 below ~10 eV proceeds via two distinct processes: a low- ($\lesssim$1 eV) and a high- (~4 to 10 eV) energy one. The former process is due to a nuclear-excited Feshbach resonance[4,6,7] leading to the formation of O_2^-, while the latter could be due to an electron-excited Feshbach resonance and it leads to the production of O^- from O_2. Both processes have been studied extensively (see ref 4), the former predominantly in electron-scattering experiments and in low-pressure ($\lesssim$1 atm) swarm experiments and the latter with mass spectrometric techniques.

The electron affinity of the O_2 molecule is 0.44 eV (see ref 4), and the O_2^{-*} formed at low energies belongs to the group of transient molecular negative ions referred to as moderately short-lived[4] (lifetimes, τ, ranging from ~10^{-12} to ~10^{-6} s) and hence it can be stabilized collisionally in a high-pressure swarm experiment. In this section we summarize and discuss the effects of the density of N_2, C_2H_4, and C_2H_6 on the rate of attachment of slow (<1 eV) electrons to O_2. All data discussed were taken at ~298 K.

A. Rates of Attachment of Slow Electrons to O_2 in High Densities of N_2, C_2H_4, and C_2H_6

The rate of attachment of slow electrons to O_2 as a function of the mean electron energy $\langle\epsilon\rangle$ and nitrogen pressure, P_{N_2}, is shown in Figure 1. The rate is seen to increase, and the functions $(\alpha w)_0$ vs. $\langle\epsilon\rangle$ are seen to shift gradually to lower energies with increasing N_2 pressure. For each P_{N_2} the maximum value of $(\alpha w)_0$ is attained at $\langle\epsilon\rangle \simeq 0.04$ eV.

Similar results have been observed[3] for O_2 in the C_2H_4 and the C_2H_6 media. These are shown in Figure 2. In this figure, $\langle\epsilon\rangle$ was taken equal to $\frac{3}{2}(eD_L/\mu)$, where e is the electron charge and D_L/μ is the ratio of the lateral electron diffusion coefficient to electron mobility; also changes in w with pressure were taken into account.[3]

The drastic and varying effects of both the nature and the

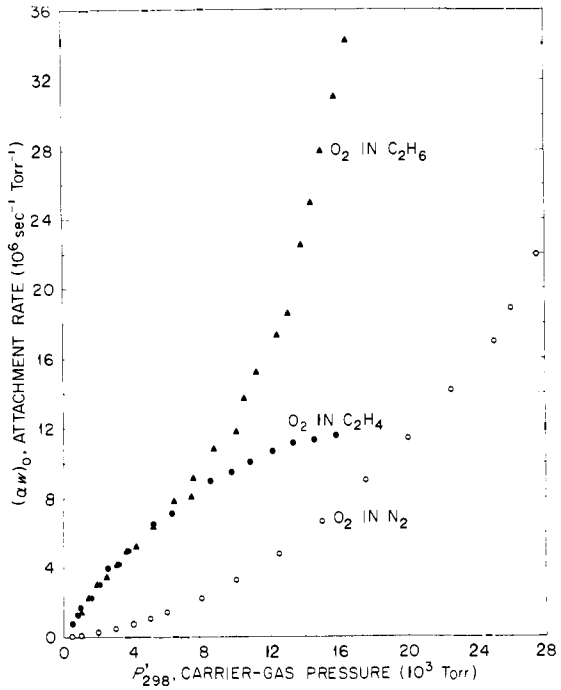

Figure 3. Attachment rate $(\alpha w)_0$ for O_2 in N_2 (○), C_2H_4 (●), and C_2H_6 (▲) as a function of the carrier-gas pressure. The data plotted are for E/P'_{298} values equal to 0.03 V cm^{-1} Torr^{-1} for N_2 and 0.1 V cm^{-1} Torr^{-1} for C_2H_4 and C_2H_6. These E/P values correspond to a mean electron energy of ~0.05 eV (from ref 3).

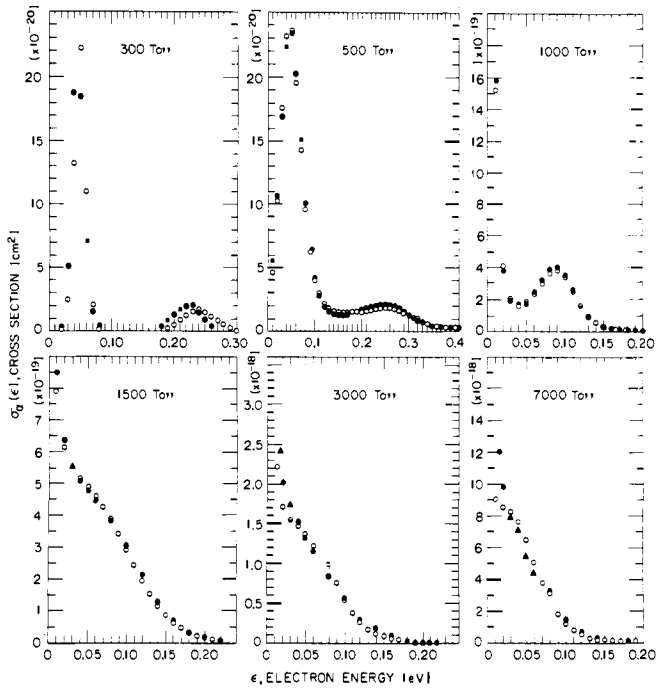

Figure 4. Cross sections for formation of O_2^- in O_2,N_2 mixtures as a function of the electron energy ϵ, at the indicated N_2 pressures. These were obtained by McCorkle, Christophorou, and Anderson[2] using the swarm-unfolding technique.[5] Note the different cross-section scales.

density of the gaseous medium on the magnitude of the attachment rate are demonstrated in Figure 3 where the attachment rate at $\langle\epsilon\rangle \simeq 0.05$ eV is plotted as a function of the pressure of the respective medium.

B. Electron Attachment Cross Sections

McCorkle et al.[2] applied the swarm-unfolding technique[5] to their data on $(\alpha w)_0$ vs. $\langle\epsilon\rangle$ in N_2 and determined the absolute attachment cross sections, $\sigma_a(\epsilon)$ for O_2^- formation in N_2 as a function of P_{N_2} shown in Figure 4. Although there may be some uncertainty as to the magnitude of these cross sections, two distinct features are clear: (i) the structure in the cross-section functions for $P_{N_2} < 1000$ Torr and (ii) the gradual shift of the cross-section function toward thermal energies with increasing N_2 density.

The structure in $\sigma_a(\epsilon)$ has been ascribed[2,3,8,9] to an electron-capture process from the $v = 0$ vibrational level of O_2 to the $v' = 4$ and $v' = 5$ vibrational levels of O_2^-, i.e.,

$$e(\epsilon \simeq 0.05\text{eV}) + O_2(X^3\Sigma_g^-, v=0) \rightarrow O_2^{-*}(X^2\Pi_g, v'=4)$$

and

$$e(\epsilon \simeq 0.24\text{eV}) + O_2(X^3\Sigma_g^-, v=0) \rightarrow O_2^{-*}(X^2\Pi_g, v'=5)$$

This can be understood easily from the potential energy diagrams in Figure 5 for $O_2(X^3\Sigma_g^-)$ and $O_2^-(X^2\Pi_g)$, constructed by Boness and Schulz[10] on the basis of their electron scattering data. In determining the potential energy curve for O_2^- they took a value of 0.43 eV for the electron affinity of O_2. The energy separation between the two maxima in $\sigma_a(\epsilon)$ shown in Figure 5 is 0.2 eV, which is somewhat larger than 0.13 eV estimated by Boness and Schulz[10] from low-pressure ($<10^{-3}$ Torr) beam studies for the energy difference between the $v' = 4$ and $v' = 5$ vibrational levels of O_2^-. Similar structure has been observed in a number of other electron-scattering experiments.[11-13] Actually, each resonance peak has been shown[14] in a study using a high-resolution electron time-of-flight spectrometer to have a doublet structure, due to the spin–orbit coupling in the $^2\Pi_g$ state of O_2^-.

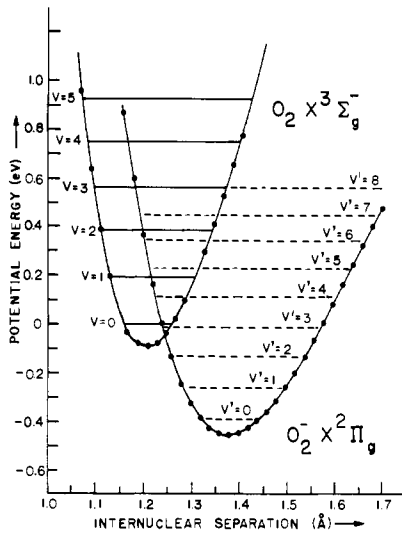

Figure 5. Potential-energy curves for O_2 and O_2^- (from ref 10).

The gradual shift of $\sigma_a(\epsilon)$ to lower energies with increasing P_{N_2} has been atrributed[3,8] to the perturbation of the potential energy curve of O_2^- by N_2 in a "hard", "sticky" collision. This perturbation may result, as in the familiar effect of solvation, in a net downward shift of the potential energy curve of O_2^-. Such changes in $\sigma_a(\epsilon)$ apparently seem so far to be characteristic of only the O_2, N_2 mixtures (see further discussion in the following section).

C. Modeling of Electron Attachment to O_2 in High Densities of N_2, C_2H_4, and C_2H_6

1. O_2 in N_2

The dependence of $\sigma_a(\epsilon)$ and $\alpha w(\langle\epsilon\rangle)$ for O_2 in N_2 on the nitrogen pressure has been explained[3,8] in terms of a model whereby N_2 is assumed (i) to act as a stabilizing third body in distant collisions and (ii) to be involved in close collisions which seriously perturb the O_2^- potential energy curve, i.e., via the two

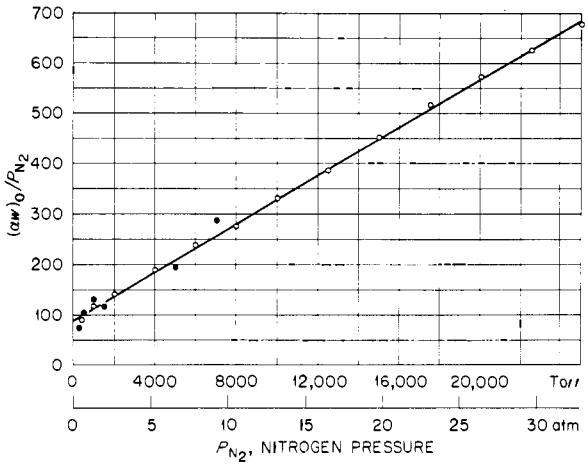

Figure 6. $(\alpha w)_0/P_{N_2}$ vs. P_{N_2}. The values of $(\alpha w)_0$ plotted are those for $\langle\epsilon\rangle \simeq 0.05$ eV, which basically correspond to the maximum value of $(\alpha w)_0$ at each P_{N_2} (see Figure 1). The solid points are from ref 2 and the open circles from ref 3.

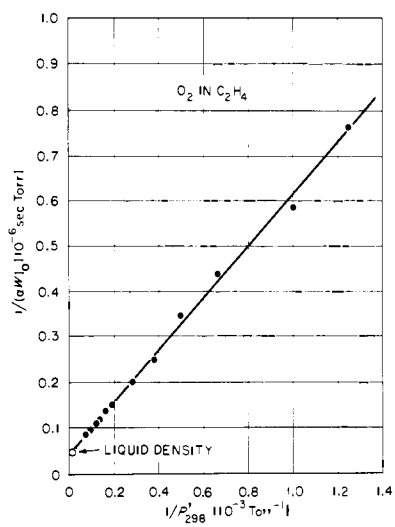

Figure 7. $1/(\alpha w)_0$ as a function of $1/P'_{298}$ for O_2 in C_2H_4. The data plotted are for $E/P'_{298} = 0.1$ V cm^{-1} Torr^{-1} (from ref 3).

Scheme I

(i) $e + O_2 \xrightarrow{k_1} O_2^{-*}$

$O_2^{-*} \xrightarrow{k_2} O_2 + e$

$O_2^{-*} + N_2 \xrightarrow{k_3} O_2^- + N_2 + \text{energy}$

$\xrightarrow{k_4} O_2 + N_2 + e$

(ii) $e + O_2 + N_2 \xrightarrow{k_5} [O_2^{-*} - N_2]$

$[O_2^{-*}\text{–}N_2] \xrightarrow{k_6} O_2 + N_2 + e$

$[O_2^{-*}\text{–}N_2] + N_2 \xrightarrow{k_7} O_2^- + 2N_2 + \text{energy}$

$\xrightarrow{k_8} O_2 + 2N_2 + e$

mechanisms in Scheme I. In mechanism ii the formation of a transient complex $[O_2^{-*}\text{–}N_2]$ is postulated which can either autoionize or lead to O_2^- upon collision with a second N_2 molecule. Calculations by Chen[15] indicated that such a complex is bound. It is to be noted that the first equation in mechanism ii is tantamount to the reverse of the fourth process in mechanism i.

On the basis of mechanisms i and ii one obtains

$$(\alpha w)_0 = \frac{k_1 k_3 n_{N_2}}{(k_3 + k_4)n_{N_2} + k_2} + \frac{k_5 k_7 n_{N_2}^2}{(k_7 + k_8)n_{N_2} + k_6} \quad (4)$$

where $k_1 \ldots k_8$ are the rate constants for the processes in mechanisms i and ii. If it is assumed that $(k_3 + k_4)n_{N_2} \ll k_2$ and $(k_7 + k_8)n_{N_2} \ll k_6$, eq 4 reduces to

$$(\alpha w)_0/P_{N_2} = A + BP_{N_2} \quad (5)$$

where A and B are constants and P_{N_2} was substituted for n_{N_2}.

A plot of $(\alpha w)_0/P_{N_2}$ vs. P_{N_2} indicated[3,8] a good agreement with the predictions of the model as exemplified by eq 5 over the pressure range $300 \leq P_{N_2} \leq 25\,000$ Torr. This is shown in Figure 6.

2. O_2 in C_2H_4

The attachment of electrons to O_2 in C_2H_4 has been found[3] to be consistent with the following simple reaction scheme

$$e + O_2 \xrightarrow{k_1'} O_2^{-*}$$

$$O_2^{-*} \xrightarrow{k_2'} O_2 + e$$

$$O_2^{-*} + C_2H_4 \xrightarrow{k_3'} O_2^- + C_2H_4 + \text{energy}$$

which predicts

$$\frac{1}{(\alpha w)_0} = \frac{1}{k_1'} + \frac{k_2'}{k_1' k_3'} \frac{1}{P'_{C_2H_4}} \quad (6)$$

The experimental data on $(\alpha w)_0$ vs. $P'_{C_2H_4}$ are plotted in the manner suggested by eq 6 in Figure 7 for $\langle\epsilon\rangle \simeq 0.05$ eV, and are seen to be consistent with eq 6. From least-squares fits to six such plots in the range 0.05 to 0.064 eV, Goans and Christophorou[3] obtained $k_1' = 2.33 \times 10^7$ s^{-1} Torr^{-1} and $k_2'/k_3' = 10\,700$ Torr. These two quantities are quite important, since the former yields an estimate of the rate of attachment of thermal electrons to O_2 at a density corresponding to that of liquid C_2H_4 and the latter can be used, as is described below, to determine the lifetime, $\tau(O_2^{-*})$, of O_2^{-*}. Indeed Figure 7 represents an excellent method of relating the data on thermal electron attachment to O_2 in gaseous C_2H_4 to "liquid-density". The lowest datum point in Figure 7 is seen to be very close to the y axis, and the intercept of the straight line can be determined quite accurately giving the value of $(\alpha w)_0$ for $P'_{C_2H_4} \to \infty$. From an extrapolation of the gaseous data, one obtains

$$[(\alpha w)_0]_{\text{intercept}} = 2.3 \times 10^7 \text{ s}^{-1} \text{ Torr}^{-1} = 4.3 \times 10^{11} \text{ s}^{-1} \text{ M}^{-1}$$

For the liquid ethylene density one determines[3]

$$[(\alpha w)_0]_{\text{liquid density}} = 3.3 \times 10^{11} \text{ s}^{-1} \text{ M}^{-1}$$

There are no data on the rate of attachment of electrons to O_2 in liquid ethylene. However, Bakale and Schmidt[16] reported a rate equal to 5×10^{11} s^{-1} M^{-1} for O_2 in neopentane and a rate equal to 5.2×10^{11} s^{-1} M^{-1} for O_2 in neohexane, both at 296 K. Similarly, Richards and Thomas[17] reported a rate equal to 1.5×10^{11} s^{-1} M^{-1} for O_2 in n-hexane at 193 K. These values (see, also, Table V in section VII) are in gratifying agreement with the one we determined above from the gaseous data. This agreement may be taken to suggest that the process of thermal electron capture by O_2 in C_2H_4 is well understood for the entire density range from the low-pressure gas to the liquid. The ethylene molecule simply acts as a stabilizing third body over the entire density range.

The quantity k_2'/k_3' gives the medium pressure at which the rate of autoionization of O_2^{-*} is equal to the rate of stabilization of O_2^{-*} via collisions with C_2H_4. This pressure we shall refer to as the critical pressure P_c. Actually P_c can be determined from Figure 7 without having been reached. To estimate $\tau(O_2^{-*})$ we

consider for the collision frequency, ν_c, between O_2^{-*} and C_2H_4 the expression

$$\nu_c = v\sigma_L N_c \quad (7)$$

in which v is the relative velocity of O_2^{-*} and C_2H_4, N_c is the number density of C_2H_4 at P_c, and σ_L is the Langevin expression for the classical cross section for spiraling collisions between O_2^{-*} and C_2H_4 given by

$$\sigma_L = (2\pi/v)(e^2\alpha/M_r)^{1/2} \quad (8)$$

where α is the static polarizability of C_2H_4, e is the electronic charge, and M_r is the reduced mass. From eq 7 and 8 we have for the average time, τ_c, between O_2^{-*},C_2H_4 collisions

$$\tau_c = \nu_c^{-1} = (2\pi N_c)^{-1}(M_r/e^2\alpha)^{1/2} \quad (9)$$

From eq 9 Goans and Christophorou[3] calculated for τ_c a value of 1.9×10^{-12} sec. Now, if p is the probability of stabilization of O_2^{-*} in each O_2^{-*},C_2H_4 collision

$$\tau(O_2^{-*}) = (k_2')^{-1} = \tau_c/p$$

For $p = 1$, $\tau(O_2^{-*}) \simeq 2$ ps. This value is in agreement with Christophorou's earlier estimate[8] and with a value[18] deduced from electron-scattering experiments, but it is considerably shorter than early estimates obtained from low-pressure (less than a few Torr) swarm work.[19-21]

3. O_2 in C_2H_6

The simplicity of the ethylene behavior is not evident in the case of ethane. Goans and Christophorou[3] were unable to find a reliable model describing the behavior of $(\alpha w)_0$ with increasing C_2H_6 density. As can be seen from Figure 8 a reaction scheme such as that for O_2 in C_2H_4 seems reasonable for $P'_{C_2H_6} \lesssim 5000$ Torr, but beyond this pressure the measured rates are much larger than those predicted on the basis of such a simple reaction scheme.

D. Electron Attachment to O_2 at Higher Energies

In the range 4 to ~10 eV, O^- is produced from O_2 in a dissociative attachment process. Although no density dependence is expected for this process, no work has been undertaken to show this. This process is not of direct interest in this paper and will not be discussed further. It is covered in ref 4.

IV. SO_2

Sulfur dioxide (SO_2) is a bent triatomic molecule with 18 valence electrons and a positive electron affinity of 1.097 eV.[22] The existing[23] experimental information shows that electrons with kinetic energies $\lesssim$10 eV attach to the SO_2 molecule via two distinct processes: a low-energy ($\lesssim$0.5 eV) one which proceeds via a nuclear-excited Feshbach resonance mechanism (eq 10a–c) and a high-energy (4–10 eV) one (eq 11a–d), which leads

$$e + SO_2 \xrightarrow{k_1} SO_2^{-*} \begin{cases} \xrightarrow{k_2} SO_2^{(*)} + e^{(\prime)} & (10a) \\ \xrightarrow[[X]]{k_{3x}} SO_2^- + \text{energy} & (10b) \\ \xrightarrow{k_4} SO_2^- + h\nu & (10c) \end{cases}$$

to dissociative attachment presumably via one or more electron-excited Feshbach resonances. In the high-energy process the transient negative ion is expected to be very short-lived, and it either autoionizes (reaction 11a) or it dissociates to negative ions and neutral fragments (reactions 11b–d). The minimum energies required for processes 11b–d are respectively 4.15, 4.52, and ~3.6 eV.[23] The dissociative attachment process will not be discussed further (see, however, section IV.E). Instead,

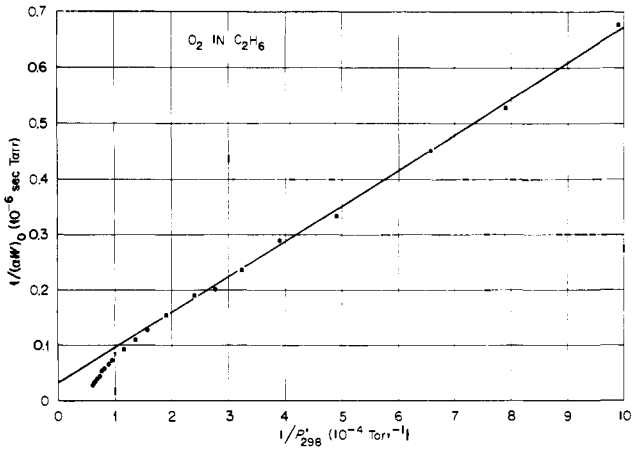

Figure 8. $1/(\alpha w)_0$ as a function of $1/P'_{298}$ for O_2 in C_2H_6. The data plotted (solid circles) are for $E/P = 0.1$ V cm^{-1} Torr^{-1}. The solid line is the prediction of eq 6 with an intercept and a slope equal to 3.2×10^{-8} sec Torr and 6.4×10^{-4} sec Torr^2, respectively (from ref 3).

$$e + SO_2 \xrightarrow{k_1'} SO_2^{-*} \begin{cases} \xrightarrow{k_2'} SO_2^{(*)} + e' & (11a) \\ \xrightarrow{k_5} O^- + SO & (11b) \\ \quad\quad SO^- + O & (11c) \\ \quad\quad S^- + O_2 & (11d) \end{cases}$$

we shall focus attention on reaction 10 which is most interesting and for which dissociation is not energetically possible. In reaction 10, k_1 is the rate constant for formation of SO_2^{-*} and k_2, k_{3x}, and k_4 are respectively the rate constants for autoionization of SO_2^{-*}, collisional stabilization of SO_2^{-*} by a second body X, and radiative stabilization of SO_2^{-*}. The symbol * indicates that the SO_2 molecule can be internally excited and the symbol ′ that the scattered electron may carry energy less than the incident one. All three channels in reaction 10 are competitive and they depend on the structure of SO_2^{-*} and the nature of the surrounding environment. Infrared studies on SO_2^- embedded in argon matrices[24] indicated tha the O–S–O valence angle is $110 \pm 5^\circ$ which is smaller than the ground-state valence O–S–O angle for the neutral molecule equal to 119.5°. This result as well as the finding[24] that the S–O stretching force constant in SO_2^- is significantly lower than that in the neutral SO_2, i.e., the S–O bonds are appreciably weaker in SO_2^-, imply that the extra (19th) electron is added to an orbital which is bonding between the two oxygen atoms and antibonding between the sulfur atom and each of the O atoms.

A. Rates of Attachment of Slow Electrons to SO_2 in High Densities of N_2 and C_2H_4

From the preceding discussion it is apparent that the attachment rates measured by Rademacher, Christophorou and Blaunstein[23] for SO_2 in N_2 and SO_2 in C_2H_4 at pressures up to 25 000 and 15 000 Torr, respectively, can be attributed to reaction 10, reaction 11 being energetically not possible. The dependence of the functions $\alpha w(\langle\epsilon\rangle)$ on $P_{C_2H_4}$ and P_{N_2} are shown in Figure 9. For both carrier gases C_2H_4 and N_2, the functions $\alpha w(\langle\epsilon\rangle)$ are seen to maximize at ~0.06 eV. The increase in αw with $P'_{C_2H_4}$ and P_{N_2} for $\langle\epsilon\rangle \simeq 0.06$ eV are dramatized in Figure 10. From both Figures 9 and 10 it is clear that for a given total pressure and energy the attachment rates for SO_2 in C_2H_4 are much larger than for SO_2 in N_2. This has been attributed[23] to the greater efficiency of the C_2H_4 molecule to stabilize the SO_2^{-*} ion in binary encounters.

B. Electron Attachment Cross Sections

The cross sections for attachment of electrons to SO_2 in N_2

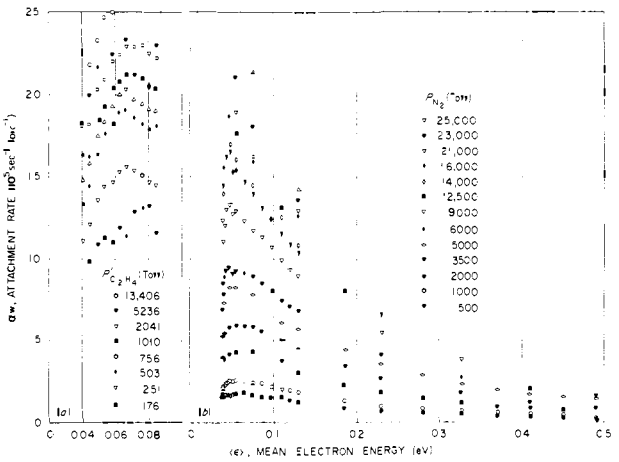

Figure 9. Attachment rate for SO_2 in C_2H_4 and N_2 as a function of the mean electron energy at the indicated total pressures (based on data in ref 23).

increase with increasing N_2 pressure and exhibit, as is shown in Figure 11, a principal maximum at ~0.06 eV and a secondary one at ~0.26 eV. Although this behavior is similar to the one we discussed earlier for O_2, the variations in the energy dependence of $\sigma_a(\epsilon)$ with P_{N_2} shown in Figure 4 for O_2 in N_2 are absent for the SO_2,N_2 data (see Figure 11); they apparently seem to be characteristic of the O_2,N_2 mixtures. Furthermore, although in the case of SO_2 it is rather difficult to assign the observed peaks to electron capture into specific vibrational levels of SO_2^-, the 0.06-eV peak in Figure 11 can be attributed to electron capture from the $v = 0$ vibrational level of SO_2 to the lowest vibrational level of SO_2^- above the $v = 0$ level of SO_2. The 0.26-eV peak is perhaps the net result of electron capture into a number of higher vibrational levels of SO_2^-. The SO_2^- ($^{32}S^{16}O_2^-$) fundamental—bending, symmetric stretch, and antisymmetric stretch—vibrations were reported[24] equal to 0.061, 0.122, and 0.129 eV, respectively.

C. Modeling of Electron Attachment to SO_2 in High Densities of N_2 and C_2H_4

1. SO_2 in C_2H_4

Rademacher, Christophorou, and Blaunstein[23] have shown that the observed electron attachment to SO_2 in C_2H_4 (Figures 9 and 10) can be treated in the same manner as the O_2 in C_2H_4 (section III.C.2) data. From plots of $1/(\alpha w)$ vs. $1/P'_{C_2H_4}$ they found that in the energy range $0.04 \leq \langle\epsilon\rangle \leq 0.09$ eV the rate of electron attachment to SO_2 in C_2H_4 when the ethylene pressure $P'_{C_2H_4} \rightarrow \infty$ is 2.3×10^6 s^{-1} Torr^{-1} and that the critical pressure is 160 Torr. Using this value for the critical pressure and the procedure outlined in section III.C.2 they found

$$\tau_{C_2H_4}(SO_2^{-*}) = 1.8 \times 10^{-10} \times 1/p \text{ (s)}$$

and since $p \leq 1$,

$$\tau_{C_2H_4}(SO_2^{-*}) \geq 1.8 \times 10^{-10} \text{ s}$$

2. SO_2 in N_2

Contrary to the case of SO_2 in C_2H_4, the attachment rates for SO_2 in N_2 attain a finite value for $P_{N_2} \rightarrow 0$; i.e., the plots αw vs. P_{N_2} display a finite intercept. If we attribute this pressure-independent component of the attachment rate to the radiative stabilization process (eq 10c), we have

$$\alpha w = \frac{k_1 k_{3x} P_{N_2}}{k_2 + k_4 + k_{3x} P_{N_2}} + \frac{k_1 k_4}{k_2 + k_4 + k_{3x} P_{N_2}} \quad (12a)$$

When $P_{N_2} \rightarrow 0$, $\alpha w \rightarrow k_1 k_4/(k_2 + k_4)$, which Rademacher, Christophorou, and Blaunstein found equal to $\sim 0.9 \times 10^5$ s^{-1} Torr^{-1} in the energy range ~0.04–0.11 eV. To test eq 12a we rewrite it as

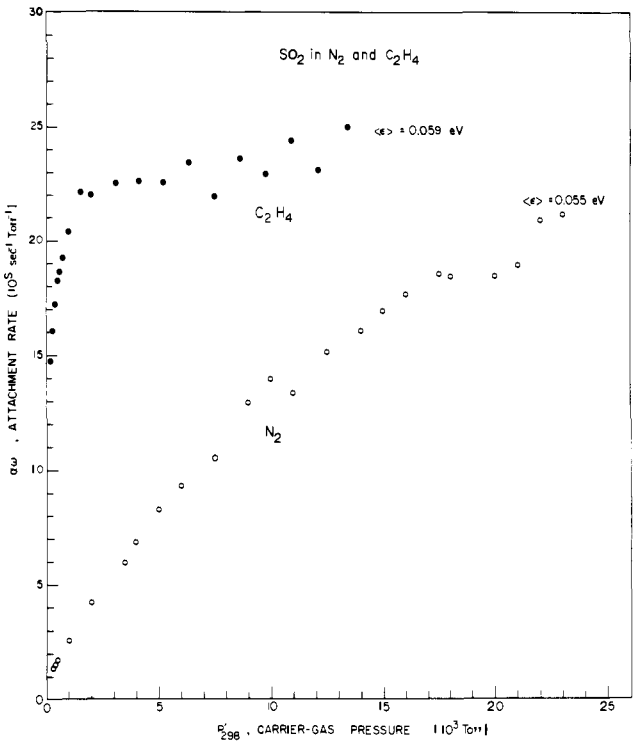

Figure 10. Attachment rate for SO_2 in C_2H_4 (●) and in N_2 (○) as a function of carrier-gas pressure for approximately the same value of $\langle\epsilon\rangle$ (~0.06 eV).

$$\frac{1}{\alpha w} = \frac{1}{k_1} + \frac{k_2}{k_1 k_4 + k_1 k_{3x} P_{N_2}} \quad (12b)$$

which reduces to

$$\frac{1}{\alpha w} = \frac{1}{k_1} + \frac{k_2}{k_1 k_{3x} P_{N_2}} \quad (13)$$

when $k_{3x} P_{N_2} \gg k_4$.

In Figure 12 the experimental data are plotted as suggested by eq 13 for $\langle\epsilon\rangle = 0.13$ eV. It is seen that, for sufficiently high values of P_{N_2}, eq 13 is obeyed. From a least-squares fit to six such plots using data for $P_{N_2} \geq 3500$ Torr in the range $0.04 \leq \langle\epsilon\rangle \leq 0.13$ eV, Rademacher, Christophorou, and Blaunstein obtained for the rate constant k_1, at infinite carrier-gas pressure, the value 2.9×10^6 s^{-1} Torr^{-1} and for the critical pressure, P_c, the value 15 000 Torr. It is interesting to see that, although k_1 is only slightly higher than its value for SO_2 in C_2H_4, the value of P_c for SO_2 in N_2 is ~94 times larger. Taking $P_c = 15\,000$ Torr, one finds through the procedure outlined in section III.C.2 that

$$\tau_{N_2}(SO_2^{-*}) \simeq 3 \times 10^{-12} \times 1/p \text{ (s)}$$

which is ~60 times shorter than that determined on the basis of the SO_2,C_2H_4 data. If this difference is attributed to differences in the value of the probability, p, of stabilization of SO_2^{-*} per collision with gas molecules for the two media, these results would indicate that $p_{C_2H_4} \simeq 60 p_{N_2}$.

Finally, if one takes for $\tau(SO_2^{-*}) = 180$ ps (i.e., the value determined from the C_2H_4 mixtures under the assumption that $p = 1$) and combines this result with the values of k_1 and $k_1 k_4/(k_2 + k_4)$ determined in this section, k_4 is found equal to 1.8×10^8 s^{-1}.

D. Extrapolation to Liquid-Phase Densities

Provided the kinetic analysis just presented is valid over the entire density range up to that for the liquid, the rates of thermal electron attachment to SO_2 at densities corresponding to those

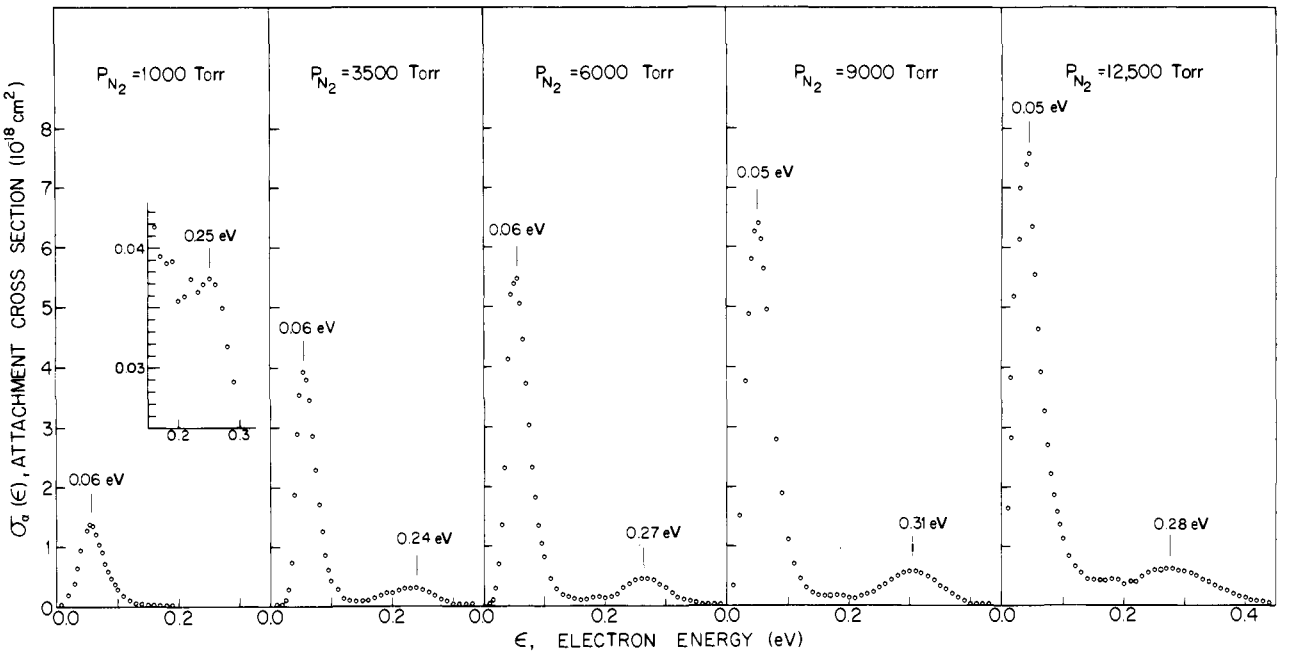

Figure 11. Attachment cross sections as a function of electron energy for SO_2 in N_2 at the indicated nitrogen pressures.

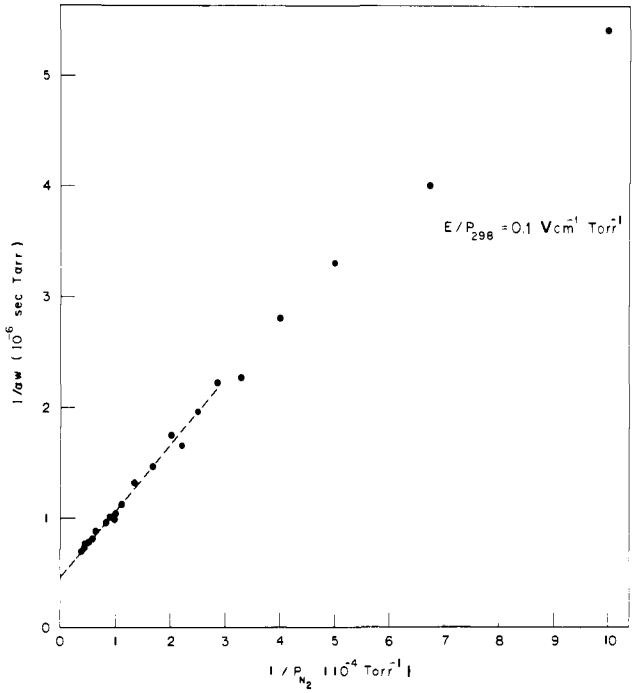

Figure 12. $1/\alpha w$ as a function of $1/P_{N_2}$ for E/P_{298} = 0.1 V cm^{-1} Torr^{-1} ($\langle\epsilon\rangle$ = 0.13 eV) (from ref 23).

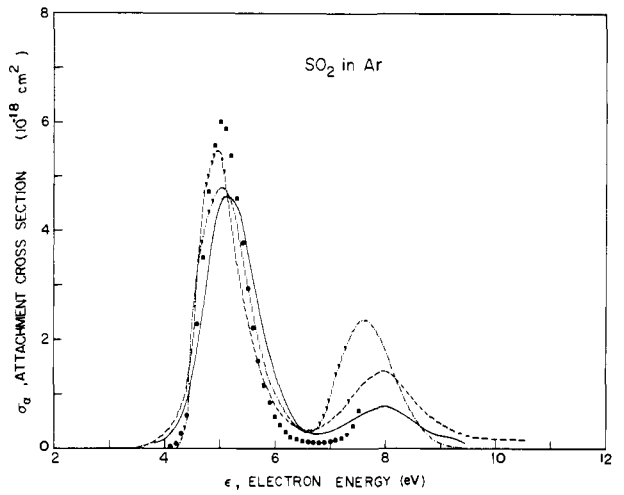

Figure 13. Attachment cross section for SO_2 in Ar obtained by Rademacher, Christophorou, and Blaunstein[23] using the swarm-unfolding[5] and swarm-beam[26] techniques and their data on $\alpha w(\langle\epsilon\rangle)$. (●) Swarm-unfolding analysis; (—), (- - -), (— • • —): swarm-beam analyses using the $\alpha w(\langle\epsilon\rangle)$ data of ref 23 for SO_2 in Ar and the negative ion yields reported, respectively, by Kraus[27] on O^- and SO^- from SO_2, by Lifshitz et al.[28] on O^- from SO_2, and by Harland and Thynne[29] on O^- from SO_2 (from ref 23).

of liquid C_2H_4 and liquid N_2 are estimated[23] to be 2.3×10^6 s^{-1} Torr^{-1} = 4.3×10^{10} s^{-1} M^{-1} and 2.9×10^6 s^{-1} Torr^{-1} = 5.4×10^{10} s^{-1} M^{-1}, respectively. There are no measurements of the rate of attachment of thermal electrons to SO_2 in liquid C_2H_4 or N_2. However, since the electron affinity of SO_2 is positive, the work of Christophorou and Blaunstein[25] would suggest that such a rate is $>10^{10}$ s^{-1} M^{-1}.

E. High-Energy Process

The cross section for dissociative attachment to SO_2 as a function of electron energy is shown in Figure 13. The cross sections obtained using different methods (see figure caption) agree reasonably well with respect to the magnitude of the first peak (~5.5×10^{-18} cm^2), but they seem to disagree appreciably as to the magnitude of the second peak at ~8 eV.

V. C_6H_6

Benzene, the simplest of the aromatics, has been the subject of many experimental and theoretical studies. The benzene molecule is known[30] to form a negative-ion resonant state with a slow electron at ~1.4 eV (see Table II in section V.C). Consistent with this finding are the results of the many theoretical calculations of its electron affinity, $(EA)_B$, which give a value for $(EA)_B < 0.0$ eV (in most cases around −1.4 eV; see ref 4 and Table II in section V.C). On the other hand, electron-attachment studies at total pressures ≲400 Torr indicated[31] that benzene captures thermal and epithermal electrons with a very low cross section. In condensed media the benzene negative ion is known to exist (see, for example, ref 32–35) and pulse-radiolysis experiments have indicated that benzene scavenges electrons in both liquid water[36-38] and alcohols[39] (see, however, ref 40).

In this section we discuss primarily the recent work of Christophorou and Goans[41] which showed that slow (≲0.3 eV)

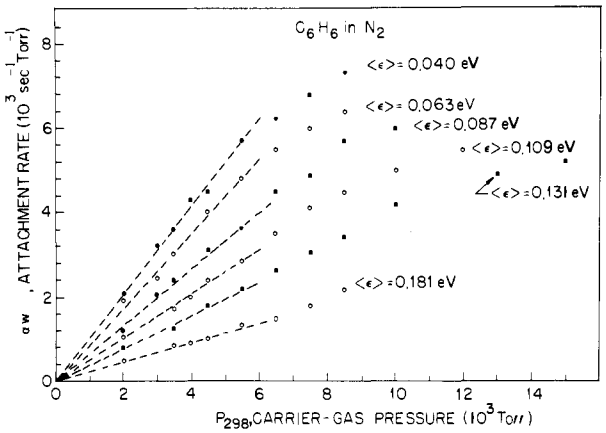

Figure 14. Attachment rate αw for C_6H_6 as a function of the carrier-gas pressure at the indicated mean electron energies. The broken lines are linear least-squares fits to the data for $P_{N_2} \leq 6000$ Torr (from ref 41).

electrons attach to benzene when the benzene molecule is in N_2 (or Ar) gas at high pressures.

A. Rates of Attachment of Slow (≲0.3 eV) Electrons to Benzene in N_2

The rates of attachment of slow electrons to benzene in N_2 (for N_2 pressures in the range 2000–15 000 Torr) measured by Christophorou and Goans[41] are shown in Figure 14 as a function of $\langle\epsilon\rangle$. They increase with increasing N_2 pressure, attain their highest value at ~0.04 eV, and decrease with increasing $\langle\epsilon\rangle$ thereafter. Furthermore, it is seen from Figure 14 that initially αw increases linearly with P_{N_2}, but as P_{N_2} increases further, αw shows a less than linear dependence on P_{N_2}. The higher the value of $\langle\epsilon\rangle$, the higher the range of N_2 pressures over which αw varies linearly with P_{N_2} This, as is discussed below, may be a consequence of the fact that the lifetime of $C_6H_6^{-*}$ decreases with increasing $\langle\epsilon\rangle$.

The data in Figure 14 were found[41] to be consistent with the simple reaction scheme

$$e + C_6H_6 \xrightarrow{k_1''} C_6H_6^{-*}$$

$$C_6H_6^{-*} \xrightarrow{k_2''} C_6H_6 + e$$

$$C_6H_6^{-*} + N_2 \xrightarrow{k_3''} C_6H_6^{-} + N_2 + \text{energy}$$

And, as was shown in similar cases earlier, plots of $1/(\alpha w)$ vs. $1/P_{N_2}$ yield $(k_1'')^{-1}$ and $k_2''/k_1''k_3''$. Indeed, from such plots in the range $0.04 \leq \langle\epsilon\rangle \leq 0.18$ eV, Christophorou and Goans[41] estimated $k_1'' \gtrsim 5 \times 10^4$ s^{-1} Torr^{-1} and, taking $k_1 = 5 \times 10^4$ s^{-1} Torr^{-1}, they determined for k_2''/k_3'' ($\equiv P_c$) the values listed in Table I. They then proceeded to determine, as discussed in section III.C.2, the lifetime $\tau(C_6H_6^{-*})$ of $C_6H_6^{-*}$ as a function $\langle\epsilon\rangle$. The values of $\tau(C_6H_6^{-*})$ are listed in Table I and were obtained by assuming that $p = 1$, but since $p \leq 1$ these represent lower limits. Despite this uncertainty, the lifetime of $C_6H_6^{-*}$ is seen to be small, in the pico- and subpicosecond range, and it decreases with increasing $\langle\epsilon\rangle$. This decrease is consistent with that for long-lived ($\tau > 10^{-6}$ s) negative ions for which the autodetachment lifetime has been predicted theoretically[4,42] and has, in many cases, been observed experimentally[4,42-44] to decrease with increasing electron energy (and thus with increasing internal energy of the metastable ion).

It is, finally, noted that as in the case of O_2 in C_2H_4 and SO_2 in C_2H_4, the plots of $(\alpha w)^{-1}$ vs. $P_{N_2}^{-1}$ for C_6H_6 in N_2 represent an excellent method for relating the gaseous data to "liquid-density" behavior. If we again make the assumption that the linear relationship found between $(\alpha w)^{-1}$ and $P_{N_2}^{-1}$ over the P_{N_2} range covered holds up to densities comparable to that of liquid N_2, we find that for $\langle\epsilon\rangle = 0.04$ eV

$$[(\alpha w)]_{\text{liq } N_2 \text{ density}} \gtrsim 5 \times 10^4 \text{ s}^{-1} \text{ Torr}^{-1} = 1 \times 10^9 \text{ s}^{-1} \text{ M}^{-1}$$

Although no measurement has been made of the rate of attachment of thermal electrons to C_6H_6 in liquid N_2, an upper limit of 1×10^9 s^{-1} M^{-1} has been placed by Bakale et al.[38] on the rate of attachment of thermal electrons to C_6H_6 in liquid *n*-hexane.

TABLE I. Values of k_2''/k_3'' ($\equiv P_c$) and $\tau(C_6H_6^{-*})$ at Various $\langle\epsilon\rangle$

$\langle\epsilon\rangle$, eV	k_2''/k_3'' ($\equiv P_c$), 10^4 Torr	$\tau(C_6H_6^{-*})$, (ps)
0.04	4.4	1
0.06	5.5	0.8
0.09	7.0	0.6
0.11	9.2	0.5
0.13	12.5	0.4
0.18	20.0	0.2

B. Evidence for Strong Collisional Detachment in $C_6H_6^{-*}$,C_2H_4 Collisions

Within the limits of their method, Christophorou and Goans[41] were unable to detect any electron attachment to benzene in mixtures with C_2H_4. They used C_6H_6 pressures up to 10 Torr and C_2H_4 pressures up to 13 000 Torr. In view of their data on C_6H_6,N_2 mixtures (see Figure 14), this was an unexpected result. For this reason, they studied C_6H_6 in binary mixtures with Ar and in tertiary mixtures with C_2H_4,N_2. Their findings for C_6H_6 in Ar substantiated their observations on C_6H_6 in N_2, while their results with the tertiary mixtures (i.e., C_6H_6, N_2, C_2H_4) supported their finding on the absence of any detectable attachment for C_6H_6 in C_2H_4. In the tertiary mixtures they observed a sharp decrease in the attachment rate for C_6H_6 in N_2 with the addition of C_2H_4. This has been attributed to a large probability of electron detachment in collisions of $C_6H_6^{-*}$ with C_2H_4. If this interpretation is correct, the rate of collisional detachment must be a strong function of the nature of the third body. Since, moreover, we have seen earlier that for O_2 and SO_2 no such profound differences were observed between the gaseous media N_2 and C_2H_4 (actually the reverse behavior was observed), it would seem that the rate for collisional detachment is also a strong function of the nature of the metastable ion itself.

C. The Electron Affinity of C_6H_6

Many theoretical calculations have been made of the electron affinity, $(EA)_B$, of benzene. The results of these are summarized in Table II, and although they are seen to vary considerably they indicate that $(EA)_B < 0$ eV. Additionally, low-energy electron-scattering experiments[30,53] revealed the existence of a negative-ion resonant (NIR) state in benzene with a maximum at ~1.4 eV and an onset at ~0.9 eV which would indicate that $(EA)_B \gtrsim -0.9$ eV. It is noted that the 1.4-eV value referred to here is actually the "vertical attachment energy," [4] i.e., the energy difference between the neutral molecule in its ground electronic, vibrational, and rotational states plus the electron at rest at infinity, and the molecular negative ion formed by addition of an electron to the neutral molecule without allowing a change in the internuclear separation of the nuclei or bond angles. It is noted, also, that the NIR referred to is a shape resonance,[61,62] having the symmetry of $^2E_{2u}$ and involving f-waves.[6]

Recent electron transmission studies[54-57] with improved energy resolution resolved vibrational structure in the lowest benzene NIR with the first vibrational level located between 1.07 and 1.15 eV (see Table II). Actually Schulz et al.[55,56] argued that their electron-scattering results, reproduced in Figure 15,

TABLE II. Literature Values of the Electron Affinity of the Benzene Molecule

Electron affinity, eV	Ref	Method[c]
−1.59	58	M
≥−1.15 ± 0.05[a]	54, 55	TR
≥−1.14 ± 0.05[a]	56	TR
≥−1.07 ± 0.07[a]	57	TR
≥−0.9 ± 0.3[b]	30, 53	TEE
−1.1 ± 0.3	59	CTS
−0.36	60	KEP
≥0	41	HPS
−1.63	45	T
−1.62	46	T
−1.42	47	T
−1.40	48–50	T
−1.15	51	T
−1.06	52	T

[a] Maximum of the first vibrational peak in the lowest shape resonance (see text). [b] Threshold of lowest shape resonance. [c] M, magnetron method; TEE, threshold-electron excitation method; TR, electron transmission in gas; CTS, charge-transfer spectra; KEP, kinetics of electron processes; HPS, high-pressure swarm experiments (see text); T, theory.

suggest that $(EA)_B = -1.15 \pm 0.05$ eV which corresponds to the lowest energy that is necessary to put an electron into the first unfilled orbital since they observed no vibrational structure below 1.15 eV. However, it should be noted that no vibrational structure was observed[56] below 2.8 eV for SO_2 either, and for this molecule the electron affinity is 1.097 eV.[22]

It thus seems that the findings of the scattering experiments are in variance with the findings of the high-pressure swarm experiments on C_6H_6 in N_2. The observation of benzene negative ions in the gas phase forces the conclusion[41] that the benzene molecule has a positive (>0 eV) electron affinity. It was pointed out[41] that $(EA)_B$ should be small in view of the short autodetachment lifetime of $C_6H_6^{-*}$ and the small cross section for its formation. It was also indicated[41] that, since electron-scattering experiments and most of the theoretical calculations are concerned with the vertical transition between B (plus an electron at rest at infinity) and B^-, and since in the swarm work one is concerned with the adiabatic value of $(EA)_B$, the requirement of their findings that $(EA)_B > 0$ eV may indicate that the potential energy surface of B^- has its minimum below that of B in a different geometry from that of B. Although this is still a possibility, scattering experiments have indicated[55,56] that in $C_6H_6^-$ and $C_6D_6^-$ the captured electron does not perturb the C–C bond appreciably. It should, of course, be kept in mind that the experimental conditions in the swarm and in the beam experiments are quite different. The much higher pressures employed in the former type of experiments could greatly affect the properties of the isolated negative ion.

VI. C_2H_5Br

Electron attachment to C_2H_5Br has been studied using both the electron-swarm[63] and the electron-beam[64] methods. Although the electron swarm study was conducted at relatively low pressures (≤1.3 atm), it still indicated the presence of a pressure-dependent component in the measured attachment rates. The electron beam study has shown that Br^- is the abundant negative ion fragment below ~3 eV.

A. Rates of Attachment of Slow (≲3 eV) Electrons to C_2H_5Br in N_2 and Ar

Recently Goans and Christophorou[65] observed significant

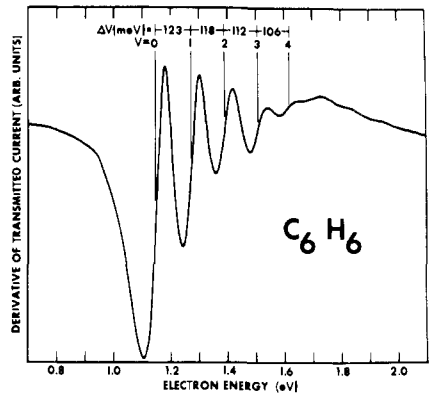

Figure 15. Derivative of the transmitted current vs. electron energy in the 1–2 eV region in benzene. The vertical lines indicate the center of each vibrational resonance. The vibrational spacings for the $^2E_{2u}$ state of $C_6H_6^-$ are shown between the vertical lines (from ref 56).

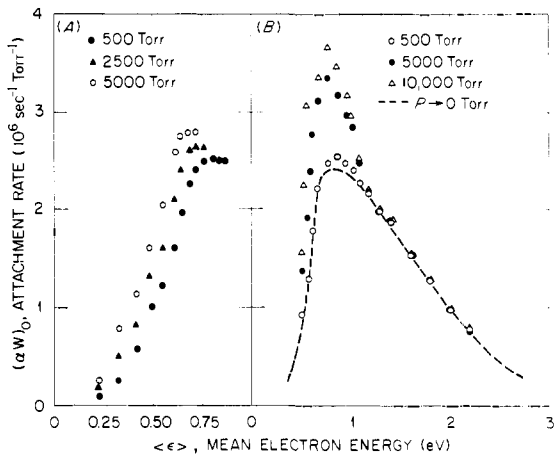

Figure 16. Attachment rate $(\alpha w)_0$ as a function of the mean electron energy for C_2H_5Br in N_2 (A) and in Ar (B) at the indicated total pressures. The broken line is the total-pressure-independent attachment rate $(\alpha w)_{0,0}$ which is attributed to dissociative attachment. The maximum value of $(\alpha w)_{0,0}$ occurs at $\langle\epsilon\rangle \simeq 0.8$ eV.

changes in both the magnitude and the energy dependence of the rate of attachment of slow (≲3 eV) electrons to C_2H_5Br in gaseous N_2 and Ar with increasing density of these media from 500 to 25 000 Torr (~33 atm) for N_2 and from 500 to 42 500 Torr (~56 atm) for Ar. These are shown in Figure 16. The rates maximize at ~0.8 eV, and their dependence on pressure is seen to be a function of the electron energy. For energies ≳1.1 eV there seems to be no appreciable dependence of the rate on the carrier-gas pressure, P_x. This, as is discussed later in this section, is a consequence of the fact that at these energies the predominant decay channel of $C_2H_5Br^{-*}$ is that of dissociation. Thus, if for a given energy the rates in Figure 16 were plotted as a function of P_x, they would be seen to increase from a finite nonzero value at $P_x = 0$ Torr initially linearly and subsequently less than linearly with P_x; at sufficiently high values of P_x (and/or energy), they would be virtually independent of pressure.

B. Reaction Scheme and Rate Constants for Electron Attachment to C_2H_5Br in High Densities of N_2 and Ar

Since it has been found[65] that both the pressure-dependent and the pressure-independent components of the attachment rate have similar energy dependences, the data in Figure 16 may be analyzed on the basis of a one-state reaction scheme[66] whereby only one state of $C_2H_5Br^-$ is assumed to be involved in the electron capture process below ~2 eV. Thus, assuming that dissociative and nondissociative electron attachments to

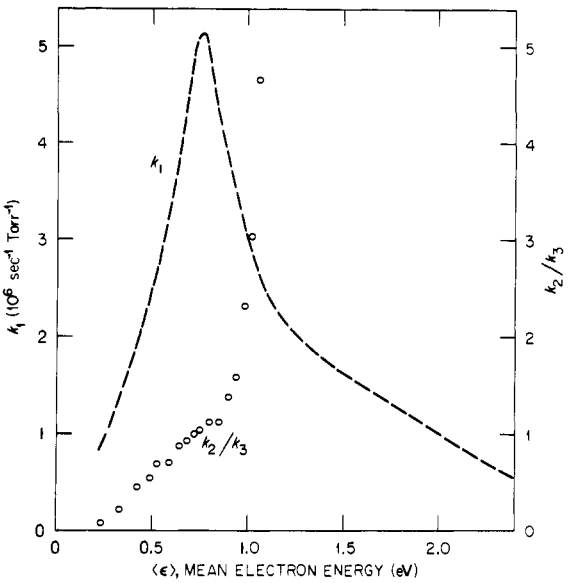

Figure 17. k_1 and k_2/k_3 as a function of $\langle\epsilon\rangle$ for C_2H_5Br (from ref 65).

C_2H_5Br proceed via a single state (which on the basis of the experimental data should be associated with a purely repulsive potential-energy curve (surface) in the Franck–Condon region and a potential-energy minimum outside it and below that of the neutral C_2H_5Br), we have the mechanism in eq 14, where X refers to either N_2 or Ar. Reaction 14 predicts that

$$e + C_2H_5Br \xrightarrow{k_1} C_2H_5Br^{-*} \begin{cases} \xrightarrow{k_2} C_2H_5 + Br^- & (14a) \\ \xrightarrow{k_3} C_2H_5Br^{(*)} + e^{(\prime)} & (14b) \\ \xrightarrow[[X]]{k_{4x}} C_2H_5Br^- + X + \text{energy} & (14c) \end{cases}$$

$$(\alpha w)_0 = \frac{k_1(k_2 + k_{4x}n_x)}{k_2 + k_3 + k_{4x}n_x} \quad (15)$$

where n_x is the number density of X which is proportional to P_x. In the limit where $P_x \rightarrow 0$, eq 15 reduces to

$$(\alpha w)_{0,0} = k_1k_2/(k_2 + k_3) \quad (16)$$

which is interpreted as the rate for dissociative attachment and is shown in Figure 16 by the broken line. From an analysis of the pressure and energy dependences of the attachment rate, Goans and Christophorou[65] calculated the absolute rate, k_1, for formation of $C_2H_5Br^{-*}$ and the ratio k_2/k_3 of the rate constant, k_2, for dissociation of $C_2H_5Br^{-*}$ to the rate constant, k_3, for autoionization of $C_2H_5Br^{-*}$. These quantities are shown in Figure 17. The energy dependence of k_1 is seen to be similar to that of $(\alpha w)_{0,0}$. At $\langle\epsilon\rangle \gtrsim 1.1$ eV, $k_1 \rightarrow (\alpha w)_{0,0}$. Furthermore, the autoionization of $C_2H_5Br^{-*}$ is seen to predominate below and the dissociation of $C_2H_5Br^{-*}$ above the peak of the resonance.

Determination of the individual rate constants k_2 and k_3 as well as of the lifetime τ $(=1/(k_2 + k_3))$ of $C_2H_5Br^{-*}$ requires an explicit knowledge of the stabilization rate $k_{4x} = k_cp$, where k_c is the collision rate of $C_2H_5Br^{-*}$ and X, and p is the probability of stabilization of $C_2H_5Br^{-*}$ in each collision with X. Upper limits to k_2 and k_3 and lower limits to τ were determined by Goans and Christophorou under the assumption that k_c is given by the classical Langevin expression for spiralling collisions and $p = 1$. The lower limit determined for τ was ~13 ps in the energy range 0.3–1.1 eV. Since, moreover, these calculations have shown that for energies below the resonance energy $k_3 \gg k_2$ and for electron energies above it $k_2 \gg k_3$, the lifetime of $C_2H_5Br^{-*}$ is primarily determined by autoionization below and by dissociation above the resonance energy.

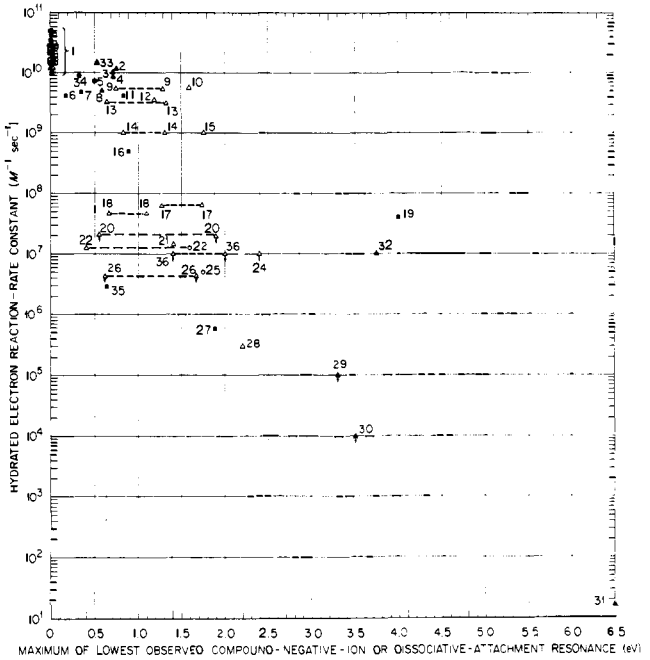

Figure 18. Hydrated electron reaction rate constant against the position of the lowest observed negative-ion or dissociative-attachment resonance (see text). The broken lines connect the positions of the double shape resonances observed for substituted and N-heterocyclic benzenes (see ref 61, 62, and 74). Numbers 2–36 identify molecules which are shown in Table III.

VII. Electron Attachment to Molecules in Gaseous and Liquid Media

A. Relevance of Quantities Describing Electron-Attachment Processes in Gases to Hydrated-Electron Reaction Rates

In an earlier study,[8,25,67] gaseous information on the parent negative ion lifetime, τ, the molecular electron affinity, $(EA)_G$, and the energy, ϵ_{max}, at which the attachment cross section peaks, has been related to hydrated electron–molecule reaction rates, R_{eaq}. The abundant data on R_{eaq} made such a comparison attractive. One of the conclusions reached in those studies was that when $(EA)_G > 0.0$ eV and/or $\tau \gtrsim 10^{-6}$ s and/or $\epsilon_{max} \lesssim \frac{3}{2}kT$, R_{eaq} attains very large ($>10^{10}$ s^{-1} M^{-1}) values, usually around 3×10^{10} s^{-1} M^{-1}. This conclusion, which allows a prediction of R_{eaq} from gaseous data, is fully upheld by the results which have appeared since.

In this section the finding is reported that R_{eaq} decreases with increasing energy, ϵ_{max}, of the lowest negative-ion resonance observed in electron-scattering experiments or in dissociative attachment studies. The available information is summarized in Figure 18 and in Table III. The points grouped together under 1 in Figure 18 are representative of molecules for which $(EA)_G > 0.0$ eV and/or $\tau \gtrsim 10^{-6}$ s and/or $\epsilon_{max} \lesssim \frac{3}{2}kT$ (see ref 8, 25, 67). The rest of the numbers in the figure identify molecules as shown in Table III.

There is a decrease in R_{eaq} with increasing position, ϵ_{max}, of the lowest negative-ion or dissociative-attachment resonance which indicates the involvement of such resonant states, and vertical transitions to them, in the formation of negative ions from molecules in aqueous solutions. It is also seen that in the case of "double resonances" [61,62] the higher lying resonance seems to correlate better with R_{eaq} than does the lower lying one. Furthermore, the data in Figure 18 seem to underscore the importance of dissociative attachment to H_2O and D_2O[82] and to suggest that the small value of R_{eaq} for H_2O and D_2O is due to this process rather than to other negative ion state(s) at a lower energy.

It seems reasonable to attribute the decrease in R_{eaq} with ϵ_{max}

TABLE III. Data on R_{eaq}, Maxima of the Lowest Observed Negative-Ion and Dissociative-Attachment Resonances, and Electron Affinity (<0 eV)

No.	Compound	R_{eaq},[68] $s^{-1}M^{-1}$	Attachment cross-section max, eV	Maximum of NIR, eV	Electron affinity, eV
2	Bromoethane	1.2×10^{10}	0.76[64]		
3	Bromobutane	1×10^{10}	0.73[64]		
4	Bromopropane	8.9×10^{9}	0.74[64]		
5	Carbon dioxide	7.7×10^{9}			≥ -0.5[69]
6	Nitrous oxide	2.4×10^{9}, 5.6×10^{9}			-0.15[70]
7	*o*-Dichlorobenzene	4.7×10^{9}	0.36[71]	~0.36[72]	
8	Nitromethane	5×10^{9}	0.6[73]		
9	Naphthalene	5.4×10^{9}		0.75; 1.3[74]	
10	Acetone	$\sim 5.8 \times 10^{9}$		1.6[75]	
11	Bromobenzene	4.3×10^{9}	0.84[71]	0.84[72]	
12	Acetaldehyde	3.5×10^{9}		1.2[75]	
13	Benzoic acid	$\sim 3.2 \times 10^{9}$		0.63; 1.33[62]	
14	Pyridine	1×10^{9}		0.84; 1.30[61]	
15	Carbon monoxide	1×10^{9}		1.75[76]	
16	Chlorobenzene	5×10^{8}	~0.9[71]	~0.9[72]	
17	Fluorobenzene	6×10^{7}		1.27; 1.74[62]	
18	Thiophenol	4.7×10^{7}		0.66; 1.10[62]	
19	Hydrogen fluoride	6×10^{7}	4[77]		
20	Aniline	$<2 \times 10^{7}$		0.55; 1.88[62]	
21	Benzene	1.4×10^{7}		1.4;[72] 1.3[78]	
22	Toluene	1.2×10^{7}		0.4; 1.60[62]	
23	Formaldehyde	$<10^{7}$			
24	Methane	$<10^{7}$		2.4[79]	
25	Ethylene	$<2.5 \times 10^{6}$; 7.6×10^{6}		1.75[78,80]	
26	Phenol	$<4 \times 10^{6}$		0.61; 1.67[62]	
27	Pyrrole	6×10^{5}			-1.88[52]
28	Urea	3×10^{5}		2.2[75]	
29	Ethanol	$<10^{5}$	~3.3[81]		
30	Methanol	$<10^{4}$	~3.5[81]		
31	Water	16	6.5[82]		
32	Hydrogen (molecular)	$<10^{7}$	3.8[4]		
33	Styrene	1.5×10^{10}			$-0.55(?)$[83]
34	Butadiene (trans)	8×10^{9}			$-0.32(?)$[83]
35	Furan	3×10^{6}			$-0.64(?)$[84]
36	Perfluoropropane	$<10^{7}$ [85]		1.4; 2.0[86]	

TABLE IV. Energies, ϵ_1 and ϵ_2, of the First and Second Maxima in the Attachment Cross Section (Figure 19), Thermal Value, $(\alpha w)_{th}$, of the Attachment Rate in Gases, and R_{eaq}

Molecule	ϵ_1, eV	ϵ_2, eV	$(\alpha w)_{th}$,[a] s^{-1} Torr^{-1}	R_{eaq},[b] s^{-1} Torr^{-1}	$(\alpha w)_{th}/R_{eaq}$
CCl_4	~0	0.2	8.5×10^{9} [c] 9×10^{9} [63] [d] 13.3×10^{9} [92] [e]	16.1×10^{5}	5280
SF_6	~0	0.32	6.7×10^{9} [c] 8.8×10^{9} [93] [d] 7.2×10^{9} [94] [f]	4.8×10^{5}	13980
CCl_3F	~0	0.35	4×10^{9} [c]	8.6×10^{5}	4650
CCl_3H	0.1	0.44	$\sim 1.3 \times 10^{8}$ [c]	8.9×10^{5}	146
c-C_4F_8	0.23	0.58	6.8×10^{8} [c] $\sim 7 \times 10^{8}$ [91] [d]	23.7×10^{5}	287
$CHClCl_2$	0.2	0.76	7.8×10^{7} [c]	10.2×10^{5}	76
CCl_2F_2	0.17	1.08	6.1×10^{7} [c] $\sim 7 \times 10^{7}$ [91] [d] 4.2×10^{7} [94] [e]	7.5×10^{5}	81

[a] For $T \simeq 298$ K. References in brackets. [b] Reference 68. [c] Present work (see text). The $\alpha w(\langle\epsilon\rangle)$ data used are from the following sources: CCl_4 [63, 89]; SF_6 [90]; CCl_3F [89]; CCl_3H [[63, 89]; c-C_4F_8 [91]; $CHClCCl_2$ [63, 89]; CCl_2F_2 [91]. [d] *Measured or extrapolated rate to* $\frac{3}{2}kT$ (0.038 eV) using the electron-swarm method. [e] Measured using the microwave method. [f] See other values in ref 4.

to a decrease in the overlap between the attachment cross section $\sigma_a(\epsilon)$ and $f(\epsilon)$, the electron-energy distribution function. However, if it is assumed that $\sigma_a(\epsilon)$ is the same in the liquid and in the gas and that $f(\epsilon)$ in the liquid is a Maxwellian function, the values of R_{eaq} at energies $\gtrsim 0.5$ eV are much too high to be explained by such an overlap. It seems that in the liquid either the electrons attain energies well in excess of thermal and/or that $\sigma_a(\epsilon)$ is shifted appreciably to lower energies as a result of solvation. Accepting the latter proposition, a shift (and a broadening due to solvent interactions) in $\sigma_a(\epsilon)$ will not only increase R_{eaq} because of the increased overlap between $f(\epsilon)$ and $\sigma_a(\epsilon)$, but also because $\sigma_a(\epsilon)$ increases with decreasing ϵ_{max}.[87] For the brominated hydrocarbons (identified by the numbers 2–4 and 11 in Table III), this shift seems to be <0.8 eV, since for these molecules $\sigma_a(\epsilon)$ peaks at ~0.8 eV and R_{eaq} is somewhat smaller than its maximum value (see Figure 18).

A comparison of the relative magnitudes of R_{eaq} and $(\alpha w)_{th}$, the thermal value of the attachment rate in the gas, is complicated by the fact that for many molecules the latter quantity is pressure dependent. Also, as a rule, two (or more) electron attachment resonances exist below ~1 eV, often within a few tenths of 1 eV of thermal, which further complicate such comparisons. In spite of these difficulties, we determined (in the manner described by Christophorou et al.[5]) the monoenergetic attachment rate $\alpha w(\epsilon)$ from published data on $\alpha w(\langle\epsilon\rangle)$ for seven molecules studied in mixtures with N_2 gas (see sources of original data in Table IV). The $\alpha w(\epsilon)$ and $\alpha w(\langle\epsilon\rangle)$ functions are presented in Figure 19 and clearly show (see also Table IV) that for all seven molecules considered, two resonances exist below ~1 eV. We used the monoenergetic attachment rates so determined (Figure 19) and calculated $(\alpha w)_{th}$ from[88]

$$(\alpha w)_{th} = \int_0^\infty \alpha w(\epsilon) f_M(\epsilon)\, d\epsilon \qquad (17)$$

where $f_M(\epsilon)$ is a Maxwellian function corresponding to $T = 298$

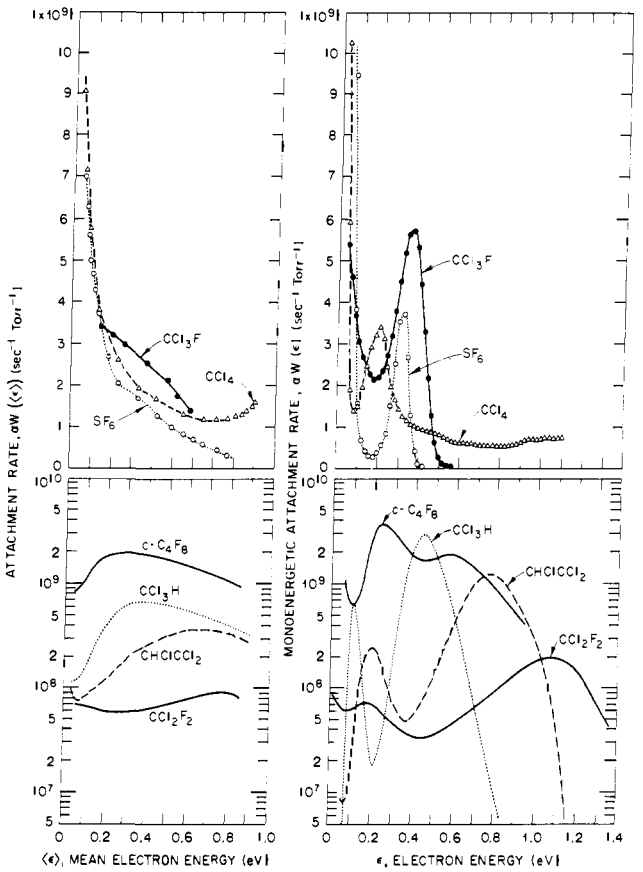

Figure 19. Attachment rate as a function of mean electron energy $\langle\epsilon\rangle$ and monoenergetic attachment rate as a function of the electron energy ϵ (see text).

K. These are listed in Table IV. It is seen from these data that when $\epsilon_{max} \simeq 0$ eV, the magnitude of $(\alpha w)_{th}$ varies from molecule to molecule by about as much as the magnitude of R_{eaq} does, but when $\epsilon_{max} > 0$ eV, R_{eaq} remains high although $(\alpha w)_{th}$ declines. This result, exemplified by the sharp decrease in the ratio $(\alpha w)_{th}/R_{eaq}$ when $\epsilon_{max} > 0$ eV, indicates a downward shift of the attachment cross section functions in the liquid as compared to the gas. The large values of the ratio $(\alpha w)_{th}/R_{eaq}$ reflect primarily the low values of R_{eaq} which are characteristic of localized-electron states whereas $(\alpha w)_{th}$ is characteristic of the free electron state in the gas phase.

B. Electron Attachment to Molecules in Nonpolar Liquids and Their Relation to Gas-Phase Data

There have been a number of measurements of the rate of attachment of quasi-free electrons to molecules dissolved in nonpolar liquids. In Table V some of these data are summarized. They have been discussed recently by Allen et al.[95] and have been elaboratred upon, among others, by Schmidt[96] and Henglein[97] in relation to the energy, V_0, of the electron in the conduction band and the electron mobility, μ_L, in the liquid. The quantity V_0 can attain positive or negative values. A positive value of V_0 indicates a localized, trapped-electron state whereas a negative value indicates an accelerated electron in a conducting, quasi-free, mobile state (V_0 can basically be regarded as the electron affinity of the medium). In the former case ($V_0 > 0$ eV) the measured electron mobility, μ_L, has been expressed[95] as

$$\mu_L = \mu_0 p(T) \tag{18}$$

and the attachment rate constant, k, for a molecule dissolved in the liquid as[95]

$$k = k'\mu_0/\mu_L \tag{19}$$

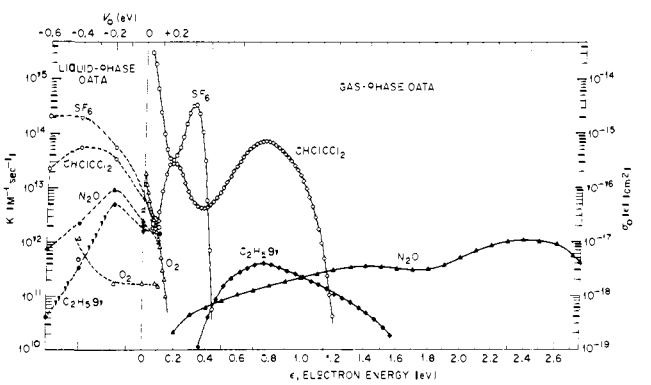

Figure 20. $k(V_0)$ and $\sigma_a(\epsilon)$ functions for a number of molecules. The $k(V_0)$ and $\sigma_a(\epsilon)$ function for CCl_4 (not plotted) are close to those for SF_6 (see Figure 19 for $\alpha w(\epsilon)$ and Table V for data on $k(V_0)$).

where μ_0 is the mean electron mobility in the mobile state, $p(T)$ is the fraction of the time the electron is in a mobile state, and k' is the measured attachment rate constant. In the latter case ($V_0 < 0$ eV), electron localization is assumed to be unimportant and $p(T) \simeq 1$; hence, $\mu_L \simeq \mu_0$ and $k \simeq k'$. In principle, the scavenger molecule can react with the electron in both the mobile and the trapped state. A zero or positive value of V_0 indicates electron localization and, with the exception of methane, is associated with a low electron mobility, while a large negative value of V_0 is associated with a high electron mobility (see Table V).

In Table V and Figure 20 gas-phase and liquid-phase data have been assembled for a number of molecules. A number of qualifying statements are given as footnotes in the table. The gas-phase cross-section functions for SF_6, $CHClCCl_2$, and N_2O were determined by the swarm-unfolding technique. The cross section for C_2H_5Br was taken from ref 64 and corresponds to a low-pressure cross section (see section VI for pressure effects on the attachment rate and thus the cross section). The cross section for O_2^- depends strongly on the gas density as it has been discussed in section III. The cross section for O_2 plotted in Figure 20 is similar in shape to that reported by Goans and Christophorou[3] for O_2 in 20 000 Torr of N_2 gas, but its magnitude was adjusted to correspond at $\epsilon = 0.05$ eV to a rate equal to 2.3×10^7 s^{-1} Torr^{-1}, i.e., to the rate of attachment estimated at this energy (see section III.C.2) for O_2 in C_2H_4 at liquid-ethylene density.

From the data in Table V and Figure 20, a number of conclusions can be drawn and a number of comments can be made, viz.:

(i) The k values in Table V are much larger than the rates of reaction of the same molecules with the hydrated electron, e_{aq}, reflecting the difference between the localized and the mobile electron states in the liquid. This is in accord with the general increase in k with decreasing V_0 (<0 eV). As stated earlier in this section, for a large negative value of V_0 the scavenger molecules react with quasi-free electron states, while for positive values of V_0 they react with quasi-free electrons for only a fraction of the time.

(ii) The magnitude of the $k(V_0)$ functions in liquids follows reasonably closely the magnitude of the $\sigma_a(\epsilon)$ functions in gases. When the electron attachment process in gases has a maximum at ~0.0 eV and it does not depend on pressure for stabilization of the metastable negative ion (i.e., when one is dealing with a dissociative attachment process or a long-lived ($\tau \gtrsim 10^{-6}$ s) negative ion), the magnitudes of the thermal attachment rates in gases are not too dissimilar from those in liquids.

(iii) The thermal attachment rate for O_2 in the gas phase compares well with the k values in various liquids although at thermal energies the O_2^{-*} ion is very short-lived ($\tau \simeq 2$ ps; see section III). This is because the effects of the medium on the attachment rate in gases have been properly considered as

TABLE V. Energies, ϵ_i, at Which the Gas-Phase Attachment Cross Sections Maximize, Thermal Values, $(\alpha w)_{th}$, of the Gas-Phpase Attachment Rates, and Attachment Rates, k, in ILIquids Which Are Characterized by V_0 and μ_L, for a Number of Molecules

Molecule	ϵ_i,[a] eV	$(\alpha w)_{th}$,[b] s^{-1} Torr^{-1}	Medium	k,[c] s^{-1} M^{-1}	V_0,[c] eV	μ_L,[c] cm^2 V^{-1} s^{-1}
SF_6	0.0; 0.32[d]	6.7×10^9	*n*-Hexane	1.9×10^{12} [e]	+0.1	0.065[e]; 0.07[f]; 0.09[g]
		[1.2×10^{14}]	Cyclohexane	4×10^{12} [e]	+0.01	0.22[e]; 0.35[g]; 0.45[h]
			2,2,4-Trimethylpentane	5.8×10^{13} [e]	−0.17	5.3[e]; 7[g]
			Neopentane	2×10^{14} [e]	−0.38	50[h]; 55[g]; 70[i,j]
			Tetramethylsilane	2.1×10^{14} [e]	−0.59	90[g]; 97[e]
$CHClCCl_2$	0.2; 0.76	7.8×10^7	*n*-Hexane	2.6×10^{12} [e]		
		[1.4×10^{12}]	2,2,4-Trimethylpentane	3.5×10^{13} [e]		
			Neopentane	5.8×10^{13} [e]		
			Tetramethylsilane	2.3×10^{13} [e]		
N_2O	0–2; 2.3[k]		*n*-Hexane	1.1×10^{12} [e]; 1.5×10^{12} [l]		
			Cyclohexane	2.4×10^{12} [e]		
			2,2,4-Trimethylpentane	9.6×10^{12} [e]		
			Neopentane	2.3×10^{12} [e]		
			Tetramethylsilane	7.5×10^{11} [e]		
C_2H_5Br	0.75[m]		*n*-Hexane	1.5 iX 10^{12} [n]		
			n-Pentane	1.6×10^{12} [n]	+0.01	0.07[f]; 0.16[g]
			Cyclohexane	2.0×10^{12} [e]		
			2,2,4-Trimethylpentane	5.1×10^{12} [e]		
			Neopentane	3.4×10^{11} [n]		
			Tetramethylsilane	4.2×10^{10} [n]		
O_c2	~0.0	2.3×10^7 [o]	*n*-Hexane	1.5×10^{11} [l,p]		
		[4.3×10^{11}]	Methylcyclohexane	1.7×10^{11} [n]	+0.08	
			Cyclohexane	1.7×10^{11} [q,p]		
			Neopentane	5×10^{11} [r]; 1.2×10^{12} [n]		
CCl_4	0.0; 0.2	8.5×10^9	*n*-Hexane	1.3×10^{12} [e]; 1.2×10^{12} [l]		
		[1.6×1^{14}]	Cyclohexane	2.7×10^{12} [e]; 4.3×10^{12} [q]		
			Neopentane	2.9×10^{13} [n]		
			Tetramethylsilane	5.4×10^{13} [n]		
CCl_3H	0.1; 0.44	~1.3×10^8	*n*-Hexane	1.5×10^{12} [l]		
		[~2.4×10^{12}]				
CH_3I	0.06	2.3×10^9	Cyclohexane	2×10^{12} [n]		
		[4.3×10^{13}]	Tetramethylsilane	1.6×10^{14} [n]		

[a] Values of ϵ at which the monoenergetic attachment rate (or the attachment cross section) has a maximum (see Table IV and Figures 19 and 20). [b] Values of the attachment rate in the gas phase for thermal electrons (see text and Table IV). The bracketed numbers are the thermal values of the attachment rate in units of s^{-1} M^{-1}. The values of ϵ_i and $(\alpha w)_{th}$ for CH_3I are based on unpublished data by R. E. Goans and L. G. Christophorou. [c] These are for temperatures between 293 and 296 K. The data on V_0 were taken from ref 98. [d] The ~0.0-eV peak is due to SF_6^- and the 0.32-eV peak is primarily due to SF_5^- (see Figure 20 and Chapter 6 of ref 4). [e] Reference 95. [f] Reference 99 (T = 300 K). [g] Reference 100. [h] Reference 101. [i] Reference 102. [j] Reference 103. [k] See Figure 20 and Chapter 6 of ref 4. The 2.3-eV peak is due to the formation of O^- from N_2O. The broad band at lower energies down to ~0.0-eV is primarily due to the production of O^- from N_2O and O^- from vibrationally excited N_2O^*, and hence it is strongly dependent on temperature.[104] At low energies N_2O^- is also formed.[104] [l] Reference 105. [m] See ref 64. See section VI for density effects on the attachment rate. [n] Reference 106. [o] This value is obtained as discussed in section III and it is for O_2 in C_2H_4 at liquid-ethylene density. [p] Beck and Thomas[107] reported much lower values than these, namely, 2.5×10^{10} and 2.3×10^{10} s^{-1} M^{-1} for O_2 in *n*-hexane and O_2 in cyclohexane, respectively. [q] Reference 108. [r] Reference 109.

TABLE VI. Lifetimes[a] of Short-Lived Parent Negative Ions and Thermal Attachment Rates for C_6H_6, O_2 and SO_2 at Densities Corresponding to Those of Liquid N_2 and Liquid C_2H_4

Negative Ion	Lifetime, ps	Energy range, eV	Electron affinity, eV	Thermal attachment rate at liquid density, s^{-1} Torr^{-1}	Comments
$C_6H_6^{-\cdot}$	1–0.2[b]	0.04–0.18	≳0.0[c]; <0[c]	≳5×10^4 [b]	From data on C_6H_6 in N_2 (400–15000 Torr)[b]
$O_2^{-\cdot}$	2[d]	Thermal	0.44[e]	2.3×10^7 [d]	From data on O_2 in C_2H_4 (750–17000 Torr)[d]
$SO_2^{-\cdot}$	200[f]	Thermal	1.097[g]	2.3×10^6 [f]	From data on SO_2 in C_2H_4 (200–15000 Torr)[f]
				2.9×10^6 [f]	From data on SO_2 in N_2 (300–25000 Torr)[f]

[a] These must be considered as lower limits since they were determined under the assumption that p = 1 (see appropriate discussion in text). [b] Reference 41. [c] See section V. [d] Reference 3. [e] Reference 111. [f] Reference 23. [g] Reference 22.

described in section III. Conversely, the observed agreement underscores the importance of the high-pressure studies in linking gaseous and liquid-phase data.

(iv) The agreement between the thermal attachment rate for O_2 in gases and the k values in liquids, coupled with the fact that the cross section for formation of O_2^- in high-pressure gases

is very narrow at thermal energies (0.0 to $\simeq$0.1 eV; see Figure 4 and footnote of Table V) and no other state leading to negative ions is known to exist below that at $\simeq$6 eV, which produces O^- ions from O_2 via dissociative attachment, provides a reasonable explanation for the low value of k for O_2 in liquids (see Table V). An analogous situation may exist for other molecules for which the cross section is similarly a very narrow resonance at thermal energies and no other state leading to negative ions exists nearby (say, within 1 or 2 eV of thermal). The cross section, for example, for perfluoromethylcyclohexane is expected to be very sharp at ~0.0 eV and for this molecule, although the thermal attachment rate in gases is large,[4] the k values for perfluoromethylcyclohexane in liquid media are low.[108]

(v) Although it has been reported[95] that the $k(V_0)$ functions "exhibit maxima and minima reminescent of those in the gas phase," it is rather difficult to relate the functions $k(V_0)$ and $\sigma_a(\epsilon)$. This can be seen from Figure 20; the $k(V_0)$ is not the mirror image of $\sigma_a(\epsilon)$. Electrons in liquids are either trapped or quasi-free while electrons in low-pressure gases are free. There is neither an accurate knowledge of the relative energies of the quasi-free and trapped electron states in the liquid, nor of the changes in the magnitude and energy dependence of the $\sigma_a(\epsilon)$ functions in going from the gas to the liquid. However, the approximate relationship of $k(V_0)$ and $\sigma_a(\epsilon)$ seen in Figure 20, and the temperature dependences of k in relation to V_0 and ϵ_{max} noted by Allen et al.,[95] distinctly indicate the significance and relevance of gas-phase data to the interpretation of liquid phase behavior. They, further, seem to indicate the involvement of vertical transitions in electron attachment to molecules dissolved in liquids in a manner analogous to that in gases.[4] For a relevant recent discussion see Funabashi and Magee.[110]

VIII. Concluding Remarks

The work on the attachment of slow electrons to molecules in high-pressure gases discussed in this paper clearly shows the importance of intermediate phase studies in understanding the effects the nature and the density of a gaseous medium have on the electron-attachment processes. It enables a deeper understanding of the competitive decay channels of metastable negative ions, an evaluation of the reaction rates for each of these channels, and a modeling of electron-attachment processes in gases which serves as a means for linking low-pressure gaseous and condensed-phase studies on electron attachment. Intermediate phase studies, also, are ideally suited for estimating the lifetimes of short-lived ($10^{-7} \lesssim \tau \lesssim 10^{-13}$ sec) negative ions—which presently cannot be measured by other methods—as well as the rates of electron attachment to molecules at liquid-phase densities. The last two quantities are listed in Table VI for C_6H_6, O_2, and SO_2. The lifetimes for the ions of these molecules are seen to lie in the pico- and subpicosecond region and seem to indicate that they increase with increasing electron affinity of the parent molecule. Incidentally, the small attachment rate for SO_2 at densities corresponding to those of liquid N_2 and C_2H_4, coupled with the narrow electron-attachment cross-section function for this molecule (see Figure 11), would suggest that the k value for SO_2 in nonpolar liquids is, as is the case for O_2, small.

The high-pressure studies are difficult in many respects. They are, however, of unique importance and should be extended to other electron–molecule (and photon–molecule) interaction processes. Such studies at our laboratory cover not only electron attachment, but also electron motion in dense gases (0.1 to ~100 atm) for temperatures $\lesssim$500 °C.

Attention is finally drawn to the evidence presented in this and a previous study[1] showing the relevance and unique significance of electron–molecule interaction processes in gases to those in liquid media. This, undoubtedly, opens the way for a more quantitative understanding of the latter.

Acknowledgment. This research was sponsored by the Energy Research and Development Administration under contract with Union Carbide Corporation.

IX. References and Notes

(1) L. G. Christophorou, *Int. J. Radiat. Phys. Chem.*, **7**, 205 (1975).
(2) D. L. McCorkle, L. G. Christophorou, and V. E. Anderson, *J. Phys. B*, **5**, 1211 (1972).
(3) R. E. Goans and L. G. Christophorou, *J. Chem. Phys.*, **60**, 1036 (1974).
(4) L. G. Christophorou, "Atomic and Molecular Radiation Physics", Wiley-Interscience, New York, N.Y., 1971.
(5) L. G. Christophorou, D. L. McCorkle, and V. E. Anderson, *J. Phys. B*, **4**, 1163 (1971).
(6) J. N. Bardsley and F. Mandl, *Rep. Prog. Phys.*, **31** (2), 471 (1968).
(7) (a) G. J. Schulz, *Rev. Mod. Phys.*, **45**, 423 (1973). (b) In contrast to this interpretation the vibrational structure of the O_2^- at these low energies has been ascribed [A. Herzenberg, *J. Chem. Phys.*, **51**, 4942 (1969)] to low-lying shape resonances.
(8) L. G. Christophorou, *J. Phys. Chem.*, **76**, 3730 (1972).
(9) D. Spence and G. J. Schulz, *Phys. Rev A*, **5**, 724 (1972).
(10) M. J. W. Boness and G. J. Schulz, *Phys. Rev. A*, **2**, 2182 (1970). See also D. Spence and G. J. Schulz, *Ibid.*, **2**, 1802 (1970).
(11) R. L. Gray, H. H. Haselton, D. Krause, Jr., and E. A. Soltysik, "Proceedings of International Conference on the Physics of Electronic and Atomic Collisions, Amsterdam, 1971, p 347.
(12) F. Linder and H. Schmidt, *Z. Naturforsch., Teil A*, **26**, 1617 (1971).
(13) P. D. Burrow, *Chem. Phys. Lett.*, **26**, 265 (1974).
(14) J. E. Land and W. Raith, *Phys. Rev. Lett.*, **30**, 193 (1973); *Phys. Rev. A*, 9, 1592 (1974).
(15) C. Chen, private communication.
(16) G. Bakale and W. F. Schmidt, private communication.
(17) J. T. Richards and J. K. Thomas, *Chem. Phys. Lett.*, **10**, 317 (1971).
(18) F. Linder and H. Schmidt, Abstracts of the 24th Annual Gaseous Electronics Conference, Gainesville, Fla., 1971, Paper W1, p 95.
(19) A. N. Prasad, *Proc. Int. Conf. Ioniz. Phenom. Gases, 7th*, 1, 79 (1965).
(20) L. M. Chanin, A. V. Phelps, and M. A. Biondi, *Phys. Rev.*, **128**, 219 (1962).
(21) A. Herzenberg, *J. Chem. Phys.*, **51**, 4942 (1969).
(22) R. J. Celotta, R. A. Bennett, and J. L. Hall, *J. Chem. Phys.*, **60**, 1740 (1974).
(23) J. Rademacher, L. G. Christophorou, and R. P. Blaunstein, *J. Chem. Soc., Faraday Trans. 2*, 71, 1212 (1975).
(24) D. E. Milligan and M. E. Jacox, *J. Chem. Phys.*, **55**, 1003 (1971).
(25) L. G. Christophorou and R. P. Blaunstein, *Chem. Phys. Lett.*, **12**, 173 (1971).
(26) L. G. Christophorou, R. N. Compton, G. S. Hurst, and P. W. Reinhardt, *J. Chem. Phys.*, **43**, 4273 (1965).
(27) K. Kraus, *Z. Naturforsch Teil A*, **16**, 1378 (1961).
(28) C. Lifshitz, J. Agam, A. Weinberg, D. Kantor, U. Shainok, and M. Peres, *Int. J. Mass Spectrom. Ion Phys.*, 11, 243 (1973).
(29) P. Harland and J. C. J. Thynne, *J. Phys. Chem.*, **74**, 52 (1970).
(30) R. N. Compton, L. G. Christophorou, and R. H. Huebner, *Phys. Lett.*, **23**, 656 (1966).
(31) L. G. Christophorou and R. P. Blaunstein, *Radiat. Res.*, **37**, 229 (1969).
(32) T. R. Tuttle, Jr., and S. I. Weissman, *J. Am. Chem. Soc.*, **80**, 5342 (1958).
(33) G. J. Hoijtink and P. J. Zandstra, *Mol. Phys.*, **3**, 371 (1960).
(34) C. L. Gardner, *J. Chem. Phys.*, **45**, 572 (1966), and references cited therein.
(35) L. J. Giling and J. G. Kloosterboer, *Chem. Phys. Lett.*, **21**, 127 (1973).
(36) E. J. Hart and M. Anbar, "The Hydrated Electron", Wiley-Interscience, New York, N.Y., 1970.
(37) D. G. Marketos, A. Marketou-Mantaka, and G. Stein, *J. Phys. Chem.*, 78, 1987 (1974).
(38) G. Bakale, E. C. Gregg, and R. D. McCreary, *J. Chem. Phys.*, **57**, 4246 (1972).
(39) H. Ogura and W. H. Hamill, *J. Phys. Chem.*, 78, 504 (1974).
(40) E. J. Hart, K. H. Schmidt, and S. Gordon, Abstracts of Papers of the 23rd Annual Meeting of the Radiation Research Society, Miami Beach, Fla., May 11-15, 1975, Paper Cc1.
(41) L. G. Christophorou and R. E. Goans, *J. Chem. Phys.*, **60**, 4244 (1974).
(42) L. G. Christophorou, A. Hadjiantoniou, and J. G. Carter, *J. Chem. Soc., Faraday Trans. 2*, **69**, 1713 (1973).
(43) P. M. Collins, L. G. Christophorou, E. L. Chaney, and J. G. Carter, *Chem. Phys. Lett.*, **4**, 646 (1970).
(44) J. P. Johnson, D. L. McCorkle, L. G. Christophorou, and J. G. Carter, *J. Chem. Soc., Faraday Trans. 2*, **71**, 1742 (1975).
(45) R. M. Hedges and F. A. Matsen, *J. Chem. Phys.*, **28**, 950 (1958).
(46) S. Ehrenson, *J. Phys. Chem.*, **66**, 706 (1962).
(47) D. R. Scott and R. S. Becker, *J. Phys. Chem.*, **66**, 2713 (1962).
(48) N. S. Hush and J. A. Pople, *Trans. Faraday Soc.*, **51**, 600 (1955).
(49) J. R. Hoyland and L. Goodman, *J. Chem. Phys.*, **36**, 21 (1962).
(50) G. L. Caldow, *Mol. Phys.*, 18, 383 (1970).
(51) B. J. McClelland, *J. Chem. Phys.*, **46**, 4158 (1967).
(52) T. L. Kunii and H. Kuroda, *Theor. Chim. Acta*, 11, 97 (1968).
(53) R. N. Compton, R. H.Huebner, P. W. Reinhardt, and L. G. Christophorou, *J. Chem. Phys.*, **48**, 901 (1968).
(54) M. J. W. Boness, I. W. Larkin, J. B. Hasted, and L. Moore, *Chem. Phys. Lett.*, 1, 292 (1967).
(55) I. Nenner and G. J. Schulz, *J. Chem. Phys.*, **62**, 1747 (1975).
(56) L. Sanche and G. J. Schulz, *J. Chem. Phys.*, **58**, 479 (1973).
(57) I. W. Larkin and J. B. Hasted, *J. Phys. B*, **5**, 95 (1972).
(58) A. F. Gaines, J. Kay, and F. M. Page, *Trans. Faraday Soc.*, **62**, 874 (1966); A. F. Gaines and F. M. Page, *ibid.*, **59**, 1266 (1963).
(59) K. Kimura and S. Nagakura, *Mol. Phys.*, 9, 117 (1967).

(60) L. E. Lyons, *Nature (London)*, **166**, 193 (1950).
(61) M. N. Pisanias, L. G. Christophorou, J. G. Carter, and D. L. McCorkle, *J. Chem. Phys.*, **58**, 2110 (1973).
(62) L. G. Christophorou, D. L. McCorkle, and J. G. Carter, *J. Chem. Phys.*, **60**, 3779 (1974). The negative-ion resonances in this and in ref 61 have been described in terms of the incident electron going into one of the unoccupied molecular orbitals of the target molecule. The two lowest unoccupied π orbitals $e_{2u,1}$ and $e_{2u,2}$ of benzene are degenerate. The capture of the electron in either orbital results in observation of only one NIR because of this degeneracy. The perturbation introduced by substitution of a C atom with an N atom in the benzene ring—as in the N-heterocyclic benzene derivatives—or the replacement of an H atom in the benzene ring by another atom or radical—as in many substituted benzene derivatives—removes the degeneracy of the $e_{2u,1}$ and $e_{2u,2}$ orbitals and allows two low-lying NIR's, referred to in the text as "double-resonances", to be observed (see ref 61 and 62).
(63) A. A. Christodoulides and L. G. Christophorou, *J. Chem. Phys.*, **54**, 4691 (1971).
(64) L. G. Christophorou, J. G. Carter, P. M. Collins, and A. A. Christodoulides, *J. Chem. Phys.*, **54**, 4706 (1971).
(65) R. E. Goans and L. G. Christophorou, *J. Chem. Phys.*, **63**, 2821 (1975).
(66) A two-state reaction scheme is, however, plausible.[65]
(67) L. G. Christophorou, Proceedings of the Third Tihany Symposium on Radiation Chemistry, Akademiai, Budapest, 1971, p 123.
(68) Reference 36; M. Anbar and P. Neta, *Int. J. Appl. Radiat. Isotopes*, **18**, 493 (1967); L. M. Dorfman and M. S. Matheson in "Progress in Radiation Kinetics", Vol. 3, G. Porter, Ed., Pergamon Press, Oxford, 1965, p 239.
(69) C. D. Cooper and R. N. Compton, *J. Chem. Phys.*, **59**, 3550 (1973).
(70) S. J. Nalley, R. N. Compton, H. C. Schweinler, and V. E. Anderson, *J. Chem. Phys.*, **59**, 4125 (1973).
(71) L. G. Christophorou, R. N. Compton, G. S. Hurst, and P. W. Reinhardt, *J. Chem. Phys.*, **45**, 536 (1966).
(72) R. N. Compton, L. G. Christophorou, and R. H. Huebner, *Phys. Lett.*, **23**, 656 (1966).
(73) A. Di Domenico and J. L. Franklin, *Int. J. Mass Spectrom. Ion Phys.*, **9**, 171 (1972).
(74) M. N. Pisanias, L. G. Christophorou and J. G. Carter, *Chem. Phys. Lett.*, **13**, 433 (1972).
(75) W. T. Naff, R. N. Compton, and C. D. Cooper, *J. Chem. Phys.*, **57**, 1303 (1972).
(76) G. J. Schulz, *Phys. Rev. A*, **135**, 988 (1964).
(77) D. C. Frost and C. A. McDowell, *J. Chem. Phys.*, **29**, 503 (1958).
(78) H. H. Brongersma, J. A. v.d. Hart and L. J. Oosterhoff, *Proc. Nobel Symp.*, **5**, 211 (1967).
(79) M. N. Pisanias, L. G. Christophorou, and J. G. Carter, Report ORNL-TM-3904, 1972. This resonance has been observed also by two other groups of investigators: ref 54 and T. Huang and W. H. Hamill, *J. Chem. Phys.*, **78**, 2077 (1974). However, H. H. Brongersma and L. J. Oosterhoff [*Chem. Phys. Lett.*, **3**, 437 (1969)] were unable to detect it.
(80) C. R. Bowman and W. D. Miller, *J. Chem. Phys.*, **42**, 681 (1965).
(81) Von L. v. Trepka and H. Neuert, *Z. Naturforsch., Teil A*, 18, 1295 (1963).
(82) R. N. Compton and L. G. Christophorou, *Phys. Rev.*, **154**, 110 (1967).
(83) J. R. Hoyland and L. Goodman, *J. Chem. Phys.*, **36**, 12, 21 (1962).
(84) T. L. Kunii and H. Kuroda, *Theor. Chim. Acta*, 11, 97 (1968).
(85) J. Shankar, *J. Indian Chem. Soc.*, **48**, 97 (1971). This author reported for both perfluoro-*n*-hexane and perfluoro-*n*-butane a rate $<10^7$ s^{-1} M^{-1}. By analogy, we assumed that for perfluoropropane the rate is also $<10^7$ s^{-1} M^{-1}.
(86) C. Lifshitz and R. Grajower, *Int. J. Mass Spectrom. Ion Phys.*, **4**, 92 (1970).
(87) L. G. Christophorou and J. A. Stockdale, *J. Chem. Phys.*, **48**, 1956 (1968).
(88) It has to be pointed out that the determination of the thermal attachment rate in the way described here, i.e., by unfolding the monoenergetic attachment rate from data at energies greater than thermal and subsequently averaging it over a Maxwellian function, constitutes an accurate and convenient method since measurement of the rate of attachment for truly thermal electrons is rather difficult to make directly and accurately.
(89) R. P. Blaunstein and L. G. Christophorou, *J. Chem. Phys.*, **49**, 1526 (1968).
(90) L. G. Christophorou, D. L. McCorkle, and J. G. Carter, *J. Chem. Phys.*, **54**, 253 (1971).
(91) L. G. Christophorou, D. L. McCorkle, and D. Pittman, *J. Chem. Phys.*, **60**, 1183 (1974).
(92) J. M. Warman and M. C. Sauer, Jr., *Int. J. Radiat. Phys. Chem.*, **3**, 273 (1971).
(93) R. W. Fessenden and K. M. Bansal, *J. Chem. Phys.*, **53**, 3468 (1970).
(94) K. M. Bansal and R. W. Fessenden, *J. Chem. Phys.*, **59**, 1760 (1973).
(95) A. O. Allen, T. E. Gangwer, and R. A. Holroyd, *J. Phys. Chem.*, **79**, 25 (1975).
(96) W. F. Schmidt, "Electron Migration in Liquids and Glasses", Hahn-Meitner-Institut für Kernforschung, Report No. HMI-B 156, Oct 1974.
(97) A. Henglein, *Ber. Bunsenges. Phys. Chem.*, **79**, 129 (1975).
(98) R. A. Holroyd and R. L. Russell, *J. Phys. Chem.*, **78**, 2128 (1974).
(99) P. M. Minday, L. D. Schmidt, and H. T. Davis, *J. Chem. Phys.*, **54**, 3112 (1971).
(100) W. F. Schmidt and A. O. Allen, *J. Chem. Phys.*, **52**, 4788 (1970).
(101) J. P. Dodelet and G. R. Freeman, *Can. J. Chem.*, **50**, 2667 (1972).
(102) R. M. Minday, L. D. Schmidt, and H. T. Davis, *J. Phys. Chem.*, **76**, 442 (1972).
(103) G. Bakale and W. F Schmidt, *Chem. Phys. Lett.*, **22**, 164 (1973).
(104) E. L. Chaney and L. G. Christophorou, *J. Chem. Phys.*, **51**, 883 (1969).
(105) J. H. Baxendale and E. J. Rasburn, *J. Chem. Soc., Faraday Trans. 1*, **70**, 705 (1974).
(106) A. O. Allen and R. A. Holroyd, *J. Phys. Chem.*, **78**, 796 (1974).
(107) G. Beck and J. K. Thomas, *J. Chem. Phys.*, **57**, 3649 (1972).
(108) J. H. Baxendale, J. P. Keene, and E. J. Rasburn, *J. Chem. Soc., Faraday Trans. 1*, **70**, 718 (1974).
(109) G. Bakale and W. F. Schmidt, quoted in ref 96.
(110) K. Funabashi and J. L. Magee, *J. Chem. Phys.*, **62**, 4428 (1975).
(111) J. L. Pack and A. V. Phelps, *J. Chem. Phys.*, **44**, 1870 (1966).